

High-Spin States of Configuration $(1d_{5/2})_{5+,0^2}$ and $(1g_{9/2})_{9+,0^2}$ Strongly Populated by the (α, d) Reaction*

C. C. LU,† M. S. ZISMAN, AND B. G. HARVEY‡

Lawrence Radiation Laboratory, University of California, Berkeley, California 94720

(Received 19 May 1969)

The (α, d) reactions on targets of ^{13}C , ^{14}C , ^{15}N , and ^{20}Ne were studied using α -particle beams of 40.1, 46.0, 45.4, and 44.5 MeV, respectively. Angular distributions were obtained. States where the captured proton-neutron pair is in the $(1d_{5/2})_{5+,0^2}$ configuration coupled to an unperturbed target core are located and possible spin assignments are suggested. These states are ^{15}N , 13.03 MeV ($\frac{1}{2}^-$), 11.95 MeV ($\frac{3}{2}^-$); ^{16}N , 5.75 MeV ($5+$); ^{17}O , 7.74 MeV ($\frac{1}{2}^-$), 9.14 MeV ($\frac{3}{2}^-$); ^{22}Na , 1.528 MeV ($5+$). Separated isotopes ^{52}Cr , $^{54,56}\text{Fe}$, $^{58,60,62}\text{Ni}$, and $^{64,66,68}\text{Zn}$ were used as targets to study the (α, d) reaction with a 50-MeV α -particle beam. States with a probable configuration of $(1g_{9/2})_{9+,0^2}$ were located. These states are ^{54}Mn , 9.47 MeV; ^{56}Co , 8.92 MeV; ^{58}Co , 6.79 MeV; ^{60}Cu , 5.99 MeV; ^{62}Cu , 4.75 MeV; ^{64}Cu , 4.57 MeV; ^{66}Ga , 2.99 MeV; ^{68}Ga , 2.88 MeV; ^{70}Ga , 2.88 MeV. The residual-interaction energies between the proton and neutron in the configurations $(1d_{5/2})_{5+,0^2}$, $(1f_{7/2})_{7+,0^2}$, and $(1g_{9/2})_{9+,0^2}$ were derived from the excitation energies determined in the present work and previous work on $(1d_{5/2})_{5+,0^2}$ and $(1f_{7/2})_{7+,0^2}$ states. For $T_z \neq 0$ nuclides, an "interaction-model" method was proposed to extract the residual-interaction energy. The mean values of the residual-interaction energies are about -3.9 , -3.0 , and -2.2 MeV, respectively, for the three mentioned configurations. There is a slight decrease of residual-interaction energy with increasing A . These results are reproduced satisfactorily by conventional shell-model calculations. Both the interaction-model method and Talmi's shell-model calculation method were used to calculate the excitation energies of states with the $(1d_{5/2})_{5+,0^2}$ configuration. In general, the former method gives better agreement with the experimental results.

I. INTRODUCTION

PIONEERING spectroscopic studies of (α, d) reactions on nuclides with $A \leq 40$, using α -particle beam energies from 42 to 53 MeV,¹⁻³ have suggested that the most strongly populated states are those in which the captured proton and neutron enter the same shell-model state¹ and couple to the maximum angular momentum with zero isobaric spin.² The pair couples to the spin and isobaric spin of the target nuclide to give the total angular momentum and isobaric spin of the preferentially populated state. The situation can be represented by the following vector-coupling relation:

$$[\mathbf{J}_i, \mathbf{T}_i + (\mathbf{j}, \mathbf{t} + \mathbf{j}, \mathbf{t})]_{J_f, T_f = T_i},$$

where J_i, T_i are the total angular momentum and isobaric spin of the target nuclide, j, t are those of the shell-model state into which the proton and neutron are captured, and J_f, T_f are those of the final state. The allowed J_f values have the range

$$|J_i - J| \leq J_f \leq J_i + J.$$

Hence, levels with a multiplicity of $2J_i + 1$, if $J > J_i$, or $2J + 1$, if $J < J_i$, will be strongly populated.

These studies of (α, d) reactions were carried out

by Rivet *et al.*³ on target nuclides ^{12}C , $^{14,15}\text{N}$, ^{16}O , ^{20}Ne , $^{24,26}\text{Mg}$, ^{28}Si , ^{32}S , ^{40}Ar , and ^{40}Ca . The following levels of the residual nuclides were strongly populated and were assigned to the configuration

$$[J_i, T_i + (1d_{5/2})_{5+,0^2}]_{J_f, T_f = T_i};$$

^{14}N ,	9.00 MeV ($5+$),
^{16}O ,	14.39 MeV ($4+$), 14.81 MeV ($6+$), 16.24 MeV ($5+$) (Refs. 3, 4),
^{17}O ,	7.6 MeV ($\frac{1}{2}^-$), 9.0 MeV ($\frac{3}{2}^-$),
^{18}F ,	1.119 MeV ($5+$) (Ref. 5),
^{22}Na ,	1.53 MeV ($5+$),
^{26}Al ,	ground state ($5+$).

Those of $[J_i, T_i + (1f_{7/2})_{7+,0^2}]_{J_f, T_f = T_i}$ are

^{26}Al ,	8.27 MeV ($7+$),
^{28}Al ,	9.80 MeV ($7+$),
^{30}P ,	7.03 MeV ($7+$),
^{34}Cl ,	5.2 MeV ($7+$),
^{42}K ,	1.87 MeV ($7+$),
^{42}Sc ,	0.60 MeV ($7+$).

Since $J > J_i$ in all these cases, we expect a multiplicity of $2J_i + 1$ levels for each nuclide. For even-even target nuclides, where $J_i = 0$, there should be only one highly populated level. For target nuclides ^{14}N ($J_i = 1$) and ^{15}N ($J_i = \frac{1}{2}$), we expect a multiplet of three and two levels, respectively, to occur. These predictions are borne out by the experiments.

The assignments of these high-spin levels were based on three criteria: (a) largest cross section, (b) simi-

* Work was performed under the auspices of the U.S. Atomic Energy Commission.

† Present Address: Nuclear Structure Laboratory, University of Rochester, Rochester, N.Y. 14627.

‡ On leave at Centre d'Etudes Nucléaires de Saclay, France.

¹ J. Cerny, University of California Lawrence Radiation Laboratory Report No. UCRL-9714, 1961 (unpublished).

² E. J.-M. Rivet, University of California Lawrence Radiation Laboratory Report No. UCRL-11341, 1964 (unpublished).

³ E. Rivet, R. H. Pehl, J. Cerny, and B. G. Harvey, Phys. Rev. 141, 1021 (1966).

⁴ M. S. Zisman, E. A. McClatchie, and B. G. Harvey (to be published).

⁵ N. F. Mangelson, University of California Lawrence Radiation Laboratory Report No. UCRL-17732, 1967 (unpublished).

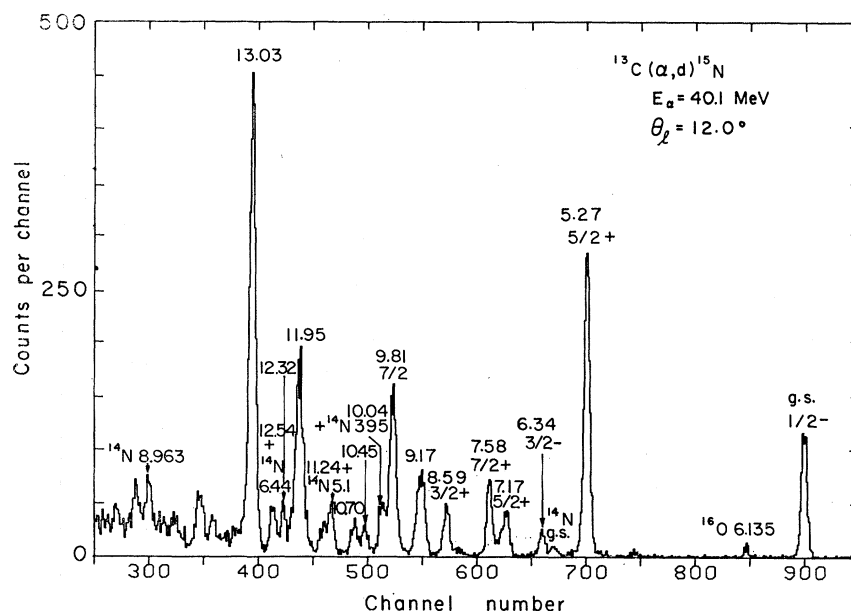


FIG. 1. Deuteron energy spectrum from the $^{13}\text{C}(\alpha, d)^{15}\text{N}$ reaction at a scattering angle of 12° (lab).

larity in the shape of angular distribution (a more or less monotonically decreasing curve with little structure), and (c) a smooth decreasing curve when $-Q_f$ was plotted against A_{res} , where $-Q_f$ is equal to the sum of $-[Q$ value of the (α, d) reaction] and the excitation energy of the assigned state, and A_{res} is the mass number of the residual nucleus ($A_{\text{target}}+2$). At the time when these assignments were made, the only spins known from other work were a possible $5+$ state at about 1 MeV in ^{18}F ; in ^{26}Al , g.s. $5+$; and in ^{42}Sc , 0.6 MeV $7+$ or $6+$. Recently, the 8.963-MeV level of ^{14}N was assigned spin $5+$,^{6,7} the 1.131-MeV level of ^{18}F was definitely established as having spin $5+$,^{7,8} and the 1.530-MeV level of ^{22}Na was assigned the spin $5+$.⁹ All these direct experimental assignments are in agreement with the predictions of the proposed model obtained from the systematics of the (α, d) reactions. These agreements strongly indicate the reliability of the model.

In order to test further the validity of the model and to extend the study to the medium-mass region ($52 \leq A \leq 70$) in a search for the existence of $[J_i, T_i + (1g_{9/2})_{9+,0^2}]_{J_f, T_f = T_i}$ states, the targets $^{13,14}\text{C}$, ^{15}N , ^{20}Ne , ^{52}Cr , $^{54,56}\text{Fe}$, $^{58,60,62}\text{Ni}$, and $^{64,66,68}\text{Zn}$ were used in the study of the (α, d) reaction with α -particle beam energies from 40 to 50 MeV. The multiplicities of the strongly populated levels were found to be in accord with the predictions. Levels with a probable $(1g_{9/2})_{9+,0^2}$ configuration were located.

⁶ R. W. Detenbeck, J. C. Armstrong, A. S. Figuera, and J. B. Marion, Nucl. Phys. **72**, 552 (1965).

⁷ A. Gallmann, F. Haas, and B. Heusch, Phys. Rev. **164**, 1257 (1967).

⁸ E. K. Warburton, Phys. Rev. **163**, 1032 (1967).

⁹ A. R. Poletti, E. K. Warburton, and J. W. Olness, Phys. Rev. **164**, 1479 (1967).

II. EXPERIMENTAL

The Berkeley 88-in. sector-focused cyclotron was used to provide α -particle beams from 40 to 50 MeV. A counter telescope consisting of two lithium-drifted silicon semiconductor detectors was used to measure the energy as well as to identify the particles. The details of this system have been described previously.^{10,3}

A cylindrical chamber approximately 3 in. in diameter and 1 in. in height was used as a gas target. The windows for entry and exit of beam particles and for the escape of secondary particles were 0.0001-in.-thick Havar foil.¹¹ A typical pressure of about 20 cm Hg was used in the gas cell.

The ^{13}C target was a CH_4 gas which contained 93.7% $^{13}\text{CH}_4$.¹² The ^{15}N target gas had an isotopic purity of 99.71%¹³ and the ^{20}Ne target gas had an isotopic purity of 98.1%.¹⁴ The solid ^{14}C target,¹⁵ which contained large amounts of ^{12}C and ^{16}O impurities, was mounted on a 2-mg/cm² gold backing.

The solid targets of medium-mass nuclides¹⁶ were prepared by vacuum evaporation of the metal onto a glass or metal plate coated with a thin layer of NaCl or Teepol¹⁷ as parting agent to permit separation of the foil from the plate. The self-supporting foils were then mounted on aluminum rectangular

¹⁰ F. S. Goulding, D. A. Landis, J. Cerny, and R. H. Pehl, Nucl. Instr. Methods **31**, 1 (1964).

¹¹ Obtained from Hamilton Watch Co., Lancaster, Pa.

¹² Obtained from Monsanto Research Corporation, Mound Laboratory, Miamisburg, Ohio.

¹³ Obtained from Isomet Corporation, Palisades Park, N.J.

¹⁴ Obtained from Mound Research Corporation.

¹⁵ The ^{14}C target was kindly loaned to us by Brookhaven National Laboratory.

¹⁶ Obtained from Union Carbide Nuclear Co., Oak Ridge National Laboratory, Oak Ridge, Tenn.

¹⁷ A detergent manufactured by Shell Oil Co., Berkeley, Calif.

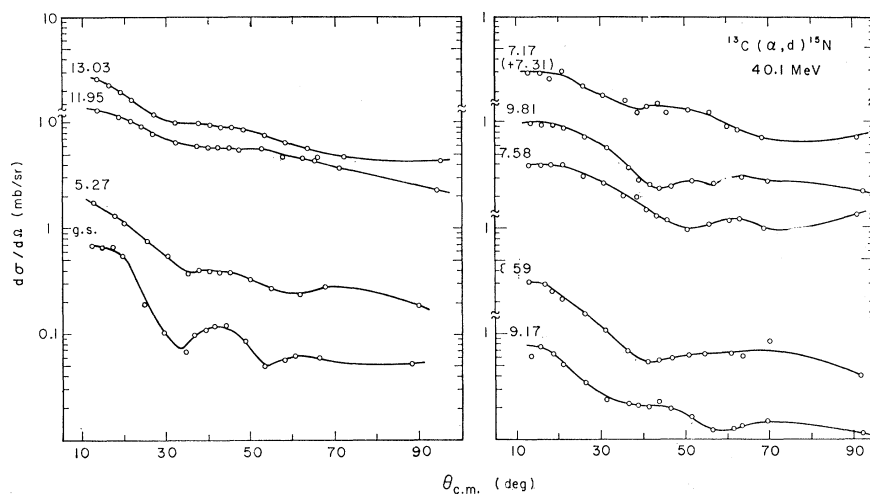


FIG. 2. Angular distributions of deuterons from the reaction $^{13}\text{C}(\alpha, d)^{15}\text{N}$ at $E_\alpha = 40.1$ MeV. The curves have no theoretical significance.

plates with $\frac{3}{4}$ -in. holes in the center. The isotopic purity of the various targets was ^{52}Cr (99.9%), ^{54}Fe (90–98%), ^{56}Fe (98–99.9%), ^{58}Ni (98–99.9%), ^{60}Ni (95–99.8%), ^{62}Ni (95–99%), ^{64}Zn (99%), ^{66}Zn (90–99%), and ^{68}Zn (95–99%).

III. RESULTS

A. $^{13}\text{C}(\alpha, d)^{15}\text{N}$

This reaction was studied with a ^{13}C methane gas target at an α -particle beam energy of 40.1 MeV. A typical spectrum taken at $\theta_{\text{lab}} = 12.0^\circ$ is shown in Fig. 1. The methane gas was found to decompose at a constant rate under irradiation of the incident beam. This effect was corrected by using the results of a monitor counter mounted at a fixed angle of 19° (lab). Angular distributions for $\theta_{\text{c.m.}} = 12.4^\circ$ – 88.2° are shown

in Fig. 2. The energy resolution [full width at half-maximum (FWHM)] was about 130 keV. The excitation energies determined here, together with the total cross sections and previously known level information, are listed in Table I.

As shown in Fig. 1, only a few levels were populated strongly. The 13.028- and 11.950-MeV levels were assigned as the doublet state with configuration

$$[(^{13}\text{C g.s.})_{1/2-, 1/2-}(1d_{5/2})_{5+, 0^2}]_{11/2-, 1/2; 9/2-, 1/2-}$$

These assignments will be discussed in detail in Sec. IV.

B. $^{14}\text{C}(\alpha, d)^{16}\text{N}$

Solid ^{14}C on a gold backing was used as the target. This reaction was studied with an α -particle beam energy of 46.0 MeV. A typical spectrum taken at

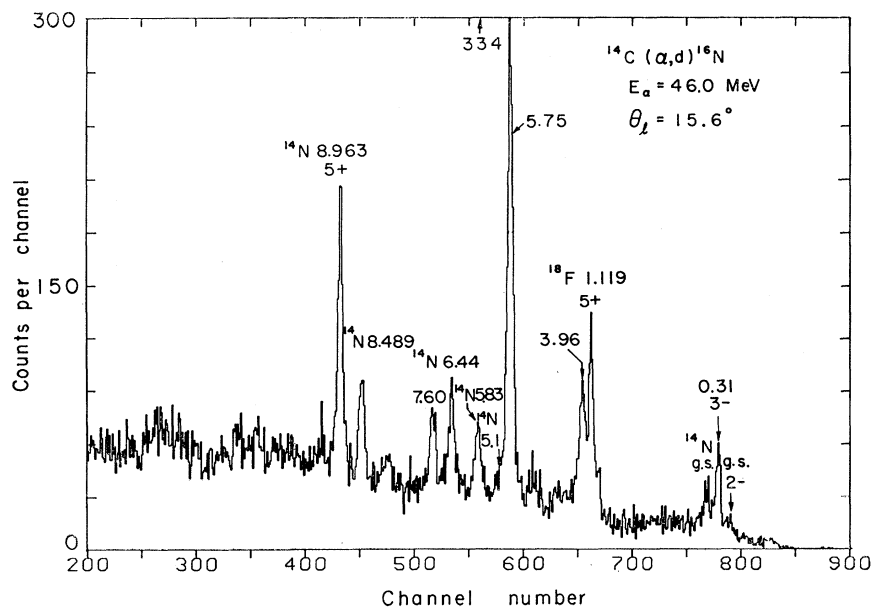


FIG. 3. Deuteron energy spectrum from the reaction $^{14}\text{C}(\alpha, d)^{16}\text{N}$ at a scattering angle of 15.6° (lab).

$\theta_{\text{lab}} = 15.6^\circ$ is shown in Fig. 3. Angular distributions for $\theta_{\text{c.m.}} = 14.5^\circ - 93.9^\circ$ are shown in Fig. 4. The energy resolution (FWHM) was about 160 keV.

The only highly populated level (at excitation 5.745 MeV) was assigned to have the dominant configuration

$$[({}^{14}\text{C g.s.})_{0+,1}(1d_{5/2})_{5+,0^2}]_{5+,1}.$$

The measured excitation energies and total cross sections, together with recent energy-level information of ${}^{16}\text{N}$, are listed in Table II.

C. ${}^{15}\text{N}(\alpha, d){}^{17}\text{O}$

Gaseous ${}^{15}\text{N}$ was used as the target. The reaction was studied with an α -particle beam energy of 45.4

TABLE I. ${}^{15}\text{N}$ levels observed in the ${}^{13}\text{C}(\alpha, d){}^{15}\text{N}$ reaction at 40.1 MeV.

Levels observed (MeV)	Previously reported levels ^{a-c}		Intensity ^d (mb)	Dominant ^e configuration
	Energy (MeV)	$J\pi$		
0	0	1/2-	0.61	$(p_{1/2})^{-1}$
5.266±0.020	5.270	5/2+	2.25	$(p_{1/2})^2 d_{5/2}$
	5.299	1/2+		
6.336±0.030	6.323	3/2-	0.70	$(p_{3/2})_{3/2}^{-1} f$
	7.154	5/2+		
7.170±0.020	7.300	3/2+	0.94	$(p_{1/2})^2 d_{5/2}$
	7.563	7/2+		
7.581±0.020	8.312	1/2+ (3/2+)	0.50	$(p_{1/2})^2 d_{5/2}$
	8.570	3/2+		
8.587±0.020	9.052	1/2+, 3/2+	1.19	$(p_{1/2})^2 d_{5/2}$
	9.155	3/2- (5/2)		
9.169±0.030	9.233	≤5/2	2.15	$(p_{1/2})^2 d_{5/2}$
	9.762	5/2-		
9.808±0.020	9.832	7/2(-)	3.20	$(d_{5/2})^2 p_{1/2}^*$
	9.929	1/2+, 3/2+		
10.451±0.020	10.074	3/2+	4.82	$(d_{5/2})^2 p_{1/2}^*$
	10.458	3/2, 5/2, 7/2		
10.698±0.020	10.548	5/2	3.20	$(d_{5/2})^2 p_{1/2}^*$
	10.710	3/2+		
11.950±0.020	10.815	3/2	3.20	$(d_{5/2})^2 p_{1/2}^*$
	11.243	>1/2-		
12.318±0.030	11.299	1/2-	4.82	$(d_{5/2})^2 p_{1/2}^*$
	11.438	1/2+		
13.028±0.020	11.616	1/2+ (T=3/2)	4.82	$(d_{5/2})^2 p_{1/2}^*$
	11.773	3/2+		
	11.885	3/2-		
	11.950	(9/2-)*		
	11.972	1/2-		
	12.103	5/2		
	12.152	3/2		
	12.333	5/2		
	12.502	5/2+ (T=3/2)		
	12.928	3/2-		
	12.93	7/2-		
	13.15	(11/2-)*		
	13.18			

^a G. W. Phillips, F. C. Young, and J. B. Marion, Phys. Rev. **159**, 891 (1967).

^b E. K. Warburton and J. W. Olness, Phys. Rev. **147**, 698 (1966); E. K. Warburton, J. W. Olness, and D. E. Alburger, *ibid.* **140**, B1202 (1965).

^c F. Ajzenberg-Selove and T. Lauritsen, Nucl. Phys. **11**, 1 (1959).

^d Range of integration: $12.4^\circ - 88.2^\circ$ (c.m.).

^e E. C. Halbert and J. B. French, Phys. Rev. **105**, 1563 (1957).

^f E. K. Warburton, P. D. Parker, and P. F. Donovan, Phys. Letters **19**, 397 (1965).

* Assigned by this work.

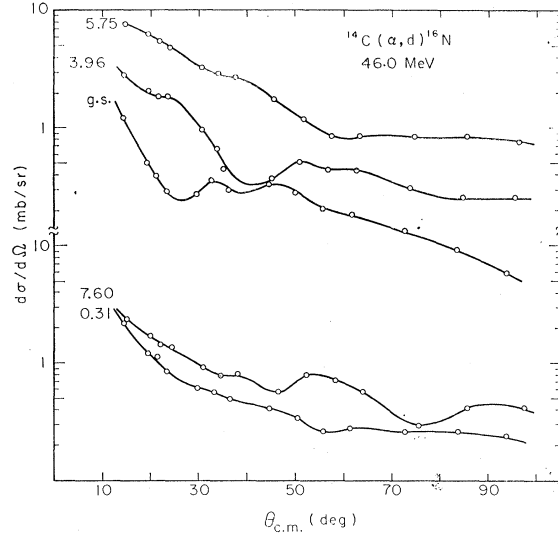


Fig. 4. Angular distributions of deuterons from the reaction ${}^{14}\text{C}(\alpha, d){}^{16}\text{N}$ at $E_\alpha = 46.0$ MeV. The curves have no theoretical significance.

MeV. A spectrum taken at $\theta_{\text{lab}} = 13.2^\circ$ is shown in Fig. 5. Angular distributions for $\theta_{\text{c.m.}} = 13.5^\circ - 82.2^\circ$ are shown in Fig. 6. The energy resolution (FWHM) was about 150 keV. The measured excitation energies and total cross sections, together with energy-level information of ${}^{17}\text{O}$, are listed in Table III.

Two strong levels at 7.742 and 9.137 MeV were assigned to have the dominant configuration

$$[({}^{15}\text{N g.s.})_{1/2-,1/2}(1d_{5/2})_{5+,0^2}]_{11/2-,1/2;9/2-,1/2}.$$

This result is in agreement with the previous (α, d) study at 47 MeV.² Better resolution was obtained in this work.

D. ${}^{20}\text{Ne}(\alpha, d){}^{22}\text{Na}$

This reaction was studied with an α -particle beam energy of 44.5 MeV and a gaseous ${}^{20}\text{Ne}$ target. Figure 7 is a spectrum taken at $\theta_{\text{lab}} = 11.2^\circ$. Angular distributions for $\theta_{\text{c.m.}} = 10.5^\circ - 57.4^\circ$ are shown in Fig. 8. The energy resolution was about 110 keV (FWHM). The measured excitation energies and total cross sections, together with energy-level information of ${}^{22}\text{Na}$, are listed in Table IV.

In general, the levels populated were the same as a previous study of this reaction.³ However, better resolution was obtained and the excitation energy studied was extended to about 16 MeV. Three levels (1.528, 7.460, and 7.874 MeV) were strongly populated. The level at 1.528 MeV was assigned to have the dominant configuration

$$[({}^{20}\text{Ne g.s.})_{0+,0}(1d_{5/2})_{5+,0^2}]_{5+,0}.$$

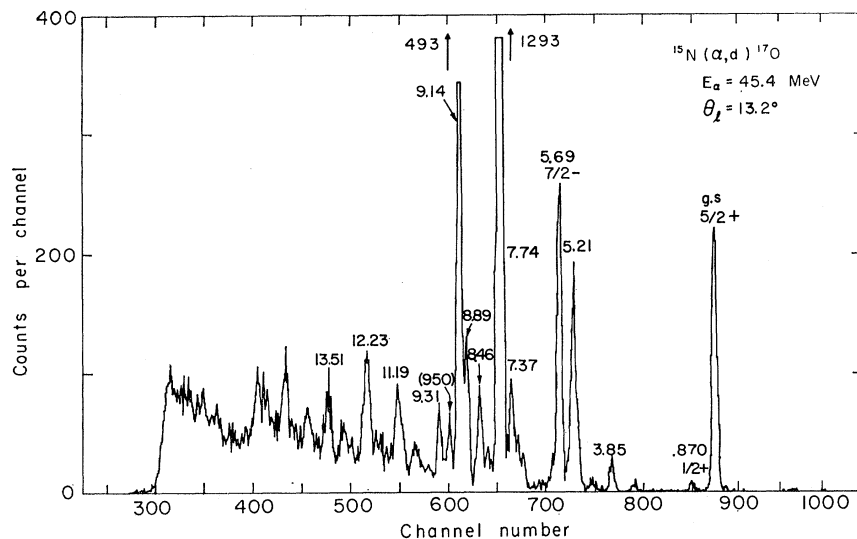


FIG. 5. Deuteron energy spectrum from the reaction $^{15}\text{N}(\alpha, d)^{17}\text{O}$ at a scattering angle of 13.2° (lab).

E. $^{52}\text{Cr}(\alpha, d)^{54}\text{Mn}$, $^{54,56}\text{Fe}(\alpha, d)^{56,58}\text{Co}$,
 $^{58,60,62}\text{Ni}(\alpha, d)^{60,62,64}\text{Cu}$, and
 $^{64,66,68}\text{Zn}(\alpha, d)^{66,68,70}\text{Ga}$

These reactions were studied with an α -particle beam energy of 50.0 MeV at four lab angles— 14° , 20° , 34° (or 35°), and 40° (or 41°). Separated isotope targets with purity ranging from 90 to 99.9% were used. The target thicknesses varied from 153 to 630 $\mu\text{g}/\text{cm}^2$. In order to stop the deuterons, a counter telescope with a ΔE counter 0.06 in. thick and an E counter 0.12 in. thick was used. The dead layer of this thick ΔE detector was the main cause of the loss of energy resolution to a typical value of 170 keV (FWHM). Spectra of deuterons from these reactions are shown in Figs. 9–17. The high selectivity in populating states by the (α, d) reaction again prevailed in this mass region. States where the captured proton-neutron pair are probably both in the $1g_{9/2}$ state and coupled to $9+$ were assigned for these nuclides. The differential cross sections for formation of these states at forward angles were about 1 mb/sr. Previously known level information for the product nuclei can be found in Refs. 18–29.

¹⁸ S. A. Hjorth, *Arkiv Fysik* **33**, 147 (1966).

¹⁹ T. A. Belote, W. E. Dorenbusch, and J. Rapaport, *Nucl. Phys.* **A109**, 666 (1968).

²⁰ M. Croissaux, E. Dally, H. Distelzwey, and C. Gehringer, *J. Phys. (Paris)* **25**, 906 (1964).

²¹ J. B. Ball and R. F. Sweet, *Phys. Rev.* **140**, B904 (1965).

²² R. H. Fulmer, A. L. McCarthy, B. L. Cohen, and R. Middleton, *Phys. Rev.* **133**, B955 (1964).

²³ R. G. Miller and R. W. Kavanagh, *Nucl. Phys.* **A94**, 261 (1967).

²⁴ S. A. Hjorth and L. H. Allen, *Arkiv Fysik* **33**, 207 (1967); W. W. Daehnick and Y. S. Park, *Bull. Am. Phys. Soc.* **12**, 1189 (1967).

²⁵ E. K. Lin and B. L. Cohen, *Phys. Rev.* **132**, 2632 (1963).

²⁶ D. von Ehrenstein and J. P. Schiffer, *Phys. Rev.* **164**, 1374 (1967).

²⁷ *Nuclear Data Sheets*, compiled by K. Way *et al.* (U.S. Government Printing Office, National Academy of Sciences–National Research Council, Washington, D.C. 20025).

²⁸ W. Menti, *Helv. Phys. Acta* **40**, 981 (1967).

²⁹ D. H. Rester, F. E. Durham, and C. M. Class, *Nucl. Phys.* **80**, 1 (1966).

IV. DISCUSSION

A. Criteria to Identify the $(1d_{5/2})_{5+,0^2}$ and $(1g_{9/2})_{9+,0^2}$ Levels

The $(1d_{5/2})_{5+,0^2}$ levels in light nuclides assigned by the present study and previous work^{2,3} are summarized

TABLE II. ^{16}N levels observed in $^{14}\text{C}(\alpha, d)^{16}\text{N}$ reaction at 46.0 MeV.

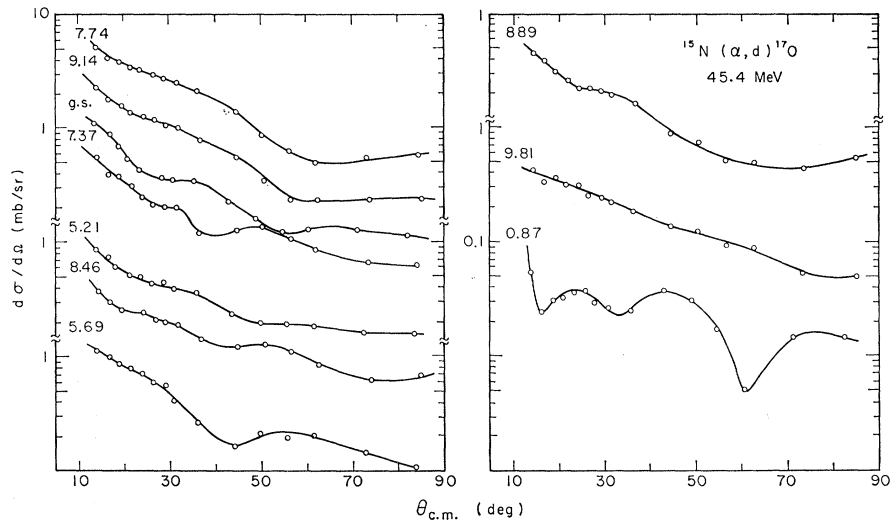
Levels observed (MeV)	Previously reported levels ^a		Intensity ^b (mb)	Dominant ^a configuration
	Energy (MeV)	$J\pi$		
0	0	2–	1.35	$(p_{1/2})^{-1}d_{5/2}$
0.307 ± 0.02	0.120	0–	2.52	$(p_{1/2})^{-1}2s_{1/2}$
	0.300	3–		$(p_{1/2})^{-1}d_{5/2}$
	0.399	1–		$(p_{1/2})^{-1}2s_{1/2}$
	3.359	1+		
3.961 ± 0.02	3.519	(0–)	3.43	
	3.957	(1, 2, 3)+		
	4.318	1+		
	4.391			
	4.725	1–		$(p_{1/2})^{-1}d_{3/2}$
	4.774	(1, 2, 3)+		
	5.053			
	5.130			
	5.150			
	5.226			
5.305	2–	$(p_{1/2})^{-1}d_{3/2}$		
5.745 ± 0.02	5.520		10.07	$(d_{5/2})_{5+,0^2}$
	5.730	(5+) ^c		$(p_{1/2})_{0+,0^2}$ ^c
	6.009	(3–)		$(p_{3/2})^{-1}d_{5/2}$
	6.167			
	6.371			
	6.422	(2–)		$(p_{3/2})^{-1}d_{5/2}$
	6.512			
	6.613			
	6.854			
	7.006			
7.599 ± 0.03	7.133		4.30	
	7.250			
	7.573			
	7.640			
	7.640			

^a P. V. Hewka, C. H. Holbrow, and R. Middleton, *Nucl. Phys.* **88**, 561 (1966).

^b Range of integration: 14.5° – 93.9° (c.m.).

^c This work.

FIG. 6. Angular distributions of deuterons from the reaction $^{15}\text{N}(\alpha, d)^{17}\text{O}$ at $E_\alpha = 45.4$ MeV. The curves have no theoretical significance.



in Table V. If from other work there are more accurately determined excitation energies for these levels, these values are listed. Angular distributions corresponding to the $(1d_{5/2})_{5+,0^2}$ levels obtained by this work are shown in Fig. 18. These angular distributions are similar to those of known $5+$ levels of previous (α, d) work. Only one of the latter, that of the 8.963-MeV $5+$ level of ^{14}N , is also shown in Fig. 18.

As stated in the Introduction, the criteria for identification of these states are that the cross section be large, that the angular distributions be similar to each other, and that the value of $-Q_f$ decrease monotonically with increasing A of the residual nucleus. (Q_f is the Q value for formation of the level.)

The large cross sections arise from the following causes:

- (a) These states have higher spins than other states

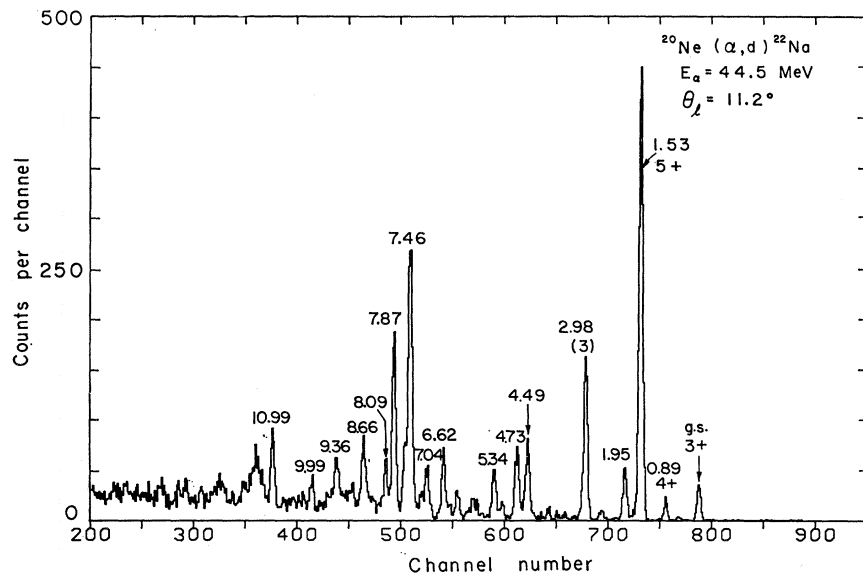
and hence the cross section is enhanced by a large statistical factor, $2J+1$.

(b) The structure factor G for these states is large.³⁰ This means roughly that the initial state plus the deuteron picked up from the α particle have large overlap with the final state.

(c) At 40–50 MeV α -particle beam energy the momentum transferred to the target ($12 \leq A \leq 24$) by the captured proton-neutron pair at the nuclear surface is about $4\hbar$, which favors capture of the two particles into the $1d_{5/2}$ shell-model state (which can give an $L=l_n+l_p=2+2=4$ transfer).³

The gross similarity of the angular distributions is caused by the fact that they are all characterized by $L=4$ transfer. The monotonically decreasing nature of the $-Q_f$ -versus- A_{res} curve can be expected because the interaction energy between the captured proton-neutron pair in the $(1d_{5/2})_{5+,0^2}$ configuration and the

FIG. 7. Deuteron energy spectrum from the reaction $^{20}\text{Ne}(\alpha, d)^{22}\text{Na}$ at a scattering angle of 11.2° (lab).



³⁰ N. K. Glendenning, Phys. Rev. 137, B102 (1965).

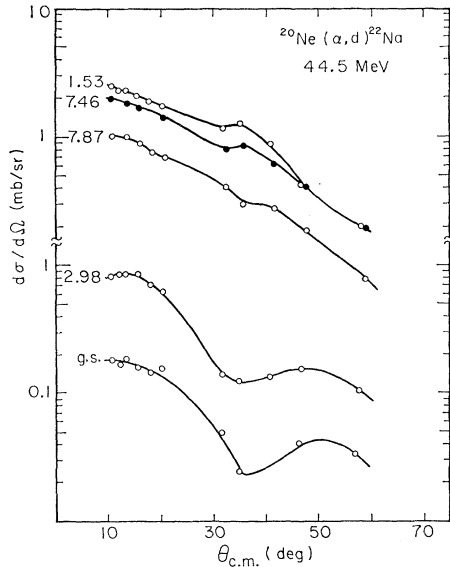


FIG. 8. Angular distributions of deuterons from the reaction $^{20}\text{Ne}(\alpha, d)^{22}\text{Na}$ at $E_\alpha = 44.5$ MeV. The curves have no theoretical significance.

target core becomes stronger when the target has more nucleons. Figure 19 shows a plot of $-Q_f$ versus A for $(1d_{5/2})_{5+,0^2}$ levels as well as for previously assigned $(1d_{5/2}, 1f_{7/2})_{6-,0}$ and $(1f_{7/2})_{7+,0^2}$ levels³ and for the $(1g_{9/2})_{9+,0^2}$ levels assigned by this work. For each configuration, a monotonically decreasing pattern is followed.

The $(1g_{9/2})_{9+,0^2}$ levels assigned by this study are listed in Table VI. Since no angular distributions were taken for these states, the assignment was based on the two criteria of a smooth monotonically decreasing $-Q_f$ -versus- A_{res} plot and largest cross section.

The causes for the relatively large cross sections for states with configuration $(1g_{9/2})_{9+,0^2}$ are the same as discussed above for the $(1d_{5/2})_{5+,0^2}$ configuration. Here, at 40–50 MeV α -particle beam energy, the momentum transferred to the target ($52 \leq A \leq 68$) by the captured proton-neutron pair at the nuclear surface is about $8\hbar$, which favors capture of the two particles into the $1g_{9/2}$ shell-model state (which can give an $L = l_n + l_p = 4 + 4 = 8$ transfer).

It was found, however, that in ^{54}Mn and ^{56}Co , it was necessary to choose the second most strongly populated level in order to obtain a smoothly varying $-Q_f$ -versus- A_{res} plot. This is not unreasonable, since the (α, t) spectra³¹ [obtained simultaneously with the (α, d) spectra] show that $1f_{7/2}$ single-particle proton capture predominates over the $1g_{9/2}$ single-particle capture in these nuclides, and thus we might expect large cross sections for levels with a configuration which includes a $1f_{7/2}$ proton to appear in the (α, d)

reaction in addition to the $(1g_{9/2})_{9+,0^2}$ levels. In the higher mass region, the (α, t) reaction³¹ shows that $1g_{9/2}$ proton capture is predominant, and here we find that the most strongly populated state should be chosen as the $(1g_{9/2})_{9+,0^2}$ level.

B. Residual-Interaction Energies between Proton and Neutron in the Configuration $(1d_{5/2})_{5+,0^2}$, $(1f_{7/2})_{7+,0^2}$, and $(1g_{9/2})_{9+,0^2}$

In the previous section we have discussed the assignment of proton-neutron two-particle excited states with the configuration $(1d_{5/2})_{5+,0^2}$. From the excitation energies of these two-particle excited states together

TABLE III. ^{17}O levels observed in $^{16}\text{N}(\alpha, d)^{17}\text{O}$ reaction at 45.4 MeV.

Levels observed (MeV)	Previously reported levels ^{a,b}			Dominant configuration
	Energy (MeV)	J_π	Intensity ^c (mb)	
0	0	5/2+	1.15	$d_{5/2}$
0.870±0.050	0.871	1/2+	0.11	$2s_{1/2}$
	3.058	(1/2-)		
3.850±0.050	3.846	5/2-	0.18	
4.566±0.050	4.555	3/2-	0.09	
	5.083	3/2+		$d_{3/2}$
5.208±0.030	5.217		1.35	
	5.378	3/2-		
5.690±0.030	5.697	7/2-	1.37	
	5.729			
	5.866	≥3/2		
	5.940	1/2-		
	6.24			
	6.38	1/2+		
	6.87			
	7.161	5/2		
	7.28	3/2+		
7.367±0.030	7.373	5/2	0.67	
	7.560	≥7/2		
	7.676	3/2		
	7.691	7/2		
	7.694	3/2		
7.742±0.020		(11/2-) ^{d,e}	6.58	$(d_{5/2})_5^2$ $p_{1/2}^{-1} d_{1/2}$
	7.91	1/2		
	8.08	3/2		
8.147±0.030	8.20	3/2	0.30	
	8.27			
	8.340	1/2		
	8.390	5/2		
8.459±0.030	8.460	7/2	0.68	
	8.493	3/2		
	(8.59)			
	8.70	3/2		
8.890±0.030	8.89	3/2	0.53	
	8.96	7/2		
	9.06			
9.137±0.030	9.15	(9/2-) ^{d,e}	2.70	$(d_{5/2})_5^2$ $p_{1/2}^{-1} d_{1/2}$
	9.20	5/2		
	9.50	7/2		
	9.73	7/2		
9.814±0.030	9.78		0.69	
	9.89	9/2		

^a F. Ajzenberg-Selove and T. Lauritsen, Nucl. Phys. 11, 1 (1959).

^b C. H. Johnson and J. L. Fowler, Phys. Rev. 162, 890 (1967).

^c Range of integration: 13.5°–82.2° (c.m.).

^d Reference 2.

^e Assigned by this work.

³¹ C. C. Lu, University of California Lawrence Radiation Laboratory Report No. UCRL-18470, 1968 (unpublished).

TABLE IV. ^{22}Na levels observed in $^{20}\text{Ne}(\alpha, d)^{22}\text{Na}$ reaction at 44.5 MeV.

Levels observed (MeV)	Previously reported levels ^{a,b}			Intensity ^c (mb)	Dominant configuration
	Energy (MeV)	$J\pi$	T		
0	0	3+	0	0.17	
	0.58305	1+	0		
	0.656	0+	1		
	0.8909	4+	0		
1.528±0.020	1.5281	5+	0	2.49	$(d_{5/2})_{5+}^{2 d,e}$
1.946±0.030	1.9359	1+		0.35	
	1.9518	(2+)	1		
	1.9835	2+, 3+			
	2.2104	1-			
2.558±0.040	2.5715	1(+), 2		0.07	
2.976±0.020	2.9686	(3)		0.70	
	3.0594	(2)			
	3.526	≥ 2			
	3.712	≥ 2			
	3.949	1			
	4.077		(1)		
	4.325				
	4.363	1, 2			
4.488±0.030				0.34	
4.733±0.020		High level density		0.50	
5.339±0.030		Spin and parity unknown		0.28	
6.274±0.020				0.22	
6.617±0.030				0.63	
7.042±0.030				0.42	
7.460±0.030	7.48 ^f			2.05	$(d_{5/2}, f_{7/2})_{6-}^d$
7.874±0.030	7.89 ^f			0.97	
8.091±0.040				0.42	
8.659±0.040				0.72	
9.356±0.040				0.59	
9.990±0.040		High level density		0.45	
10.990±0.040		Spin and parity unknown		0.69	

^a E. K. Warburton, J. W. Olness, and A. R. Poletti, Phys. Rev. 160, 938 (1967); A. R. Poletti, E. K. Warburton, J. W. Olness, and S. Hecht, *ibid.*, 162, 1040 (1967).
^b Reference 9.

^c Range of integration: 10.5°–57.4° (c.m.).
^d Reference 3.

^e Assigned by this work.

^f S. E. Arnell and E. Wernbom-Selin, Arkiv Fysik 27, 1 (1964).

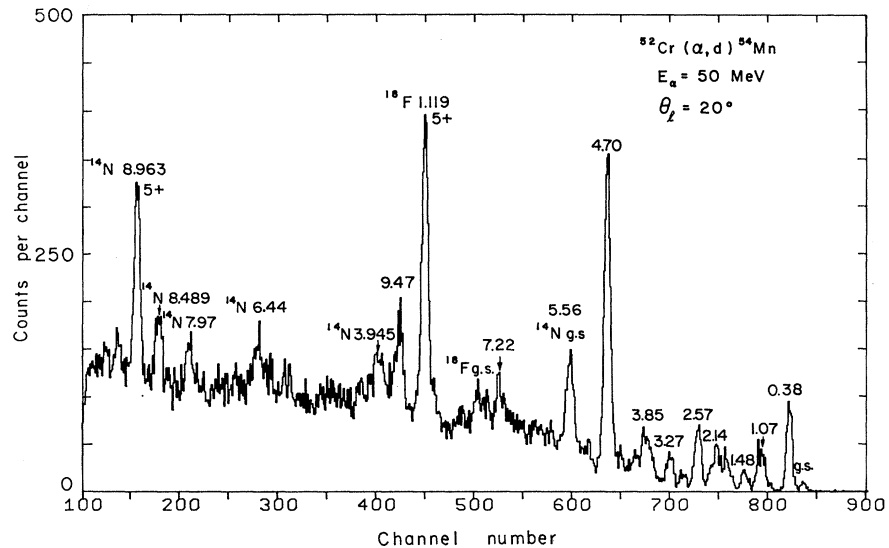


FIG. 9. Deuteron energy spectrum from the reaction $^{52}\text{Cr}(\alpha, d)^{54}\text{Mn}$ at a scattering angle of 20° (lab).

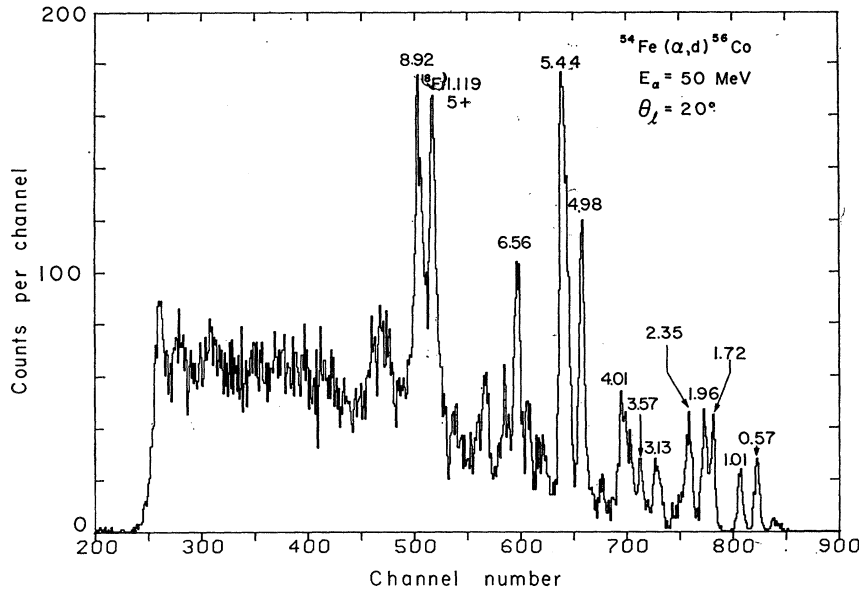


FIG. 10. Deuteron energy spectrum from the reaction $^{54}\text{Fe}(\alpha, d)^{56}\text{Co}$ at a scattering angle of 20° (lab).

with known neighboring single-particle energies, the residual-interaction energy between the proton and neutron can be calculated. The method of calculation is outlined below.

For $T_z=0$ nuclei, the calculation is simple. For example, in ^{14}N , the 8.963-MeV $5+$ level was assigned to have the configuration

$$[(^{12}\text{C core})(1d_{5/2})_{5+,0^2}]_{5+,0}$$

The total separation energy of the proton and neutron in this configuration from the ^{12}C core, denoted by S_T , is

$$S_T = S_{pn} - E^* = S_p + S_n - E(1d_{5/2})_{5+,0^2}, \quad (1)$$

where S_{pn} is the separation energy of the last proton

and neutron in the ground state of ^{14}N from the ^{12}C core, E^* is the excitation energy of the $(1d_{5/2})_{5+,0^2}$ state (equal to 8.963 MeV in this case), S_p is the separation energy of a proton in the $1d_{5/2}$ single-particle state of ^{13}N (3.56-MeV $\frac{5}{2}+$ state), S_n is the separation energy of a neutron in the $1d_{5/2}$ single-particle state of ^{13}C (3.85-MeV $\frac{5}{2}+$ state), and $E(1d_{5/2})_{5+,0^2}$ is the residual-interaction energy between the proton and the neutron in the configuration $(1d_{5/2})_{5+,0^2}$. The results of these calculations for the nuclides ^{14}N , ^{18}F , ^{22}Na , and ^{26}Al are listed in Table VII. The neighboring single-particle states used in the calculations are also tabulated. The mass table of Ref. 32 is used in calculating the separation energies. The residual-interaction energies stay fairly constant over

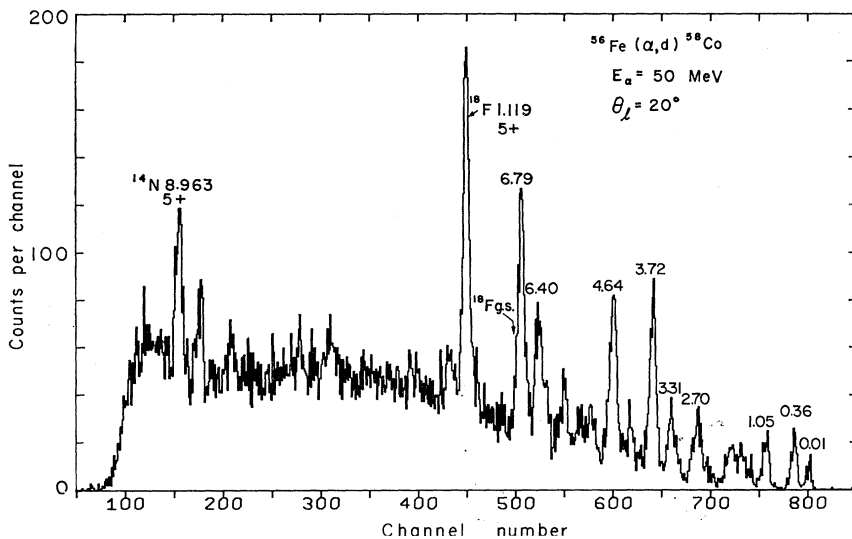


FIG. 11. Deuteron energy spectrum from the reaction $^{56}\text{Fe}(\alpha, d)^{58}\text{Co}$ at a scattering angle of 20° (lab).

³² C. Maples, G. W. Goth, and J. Cerny, Tables of Atomic Masses (unpublished).

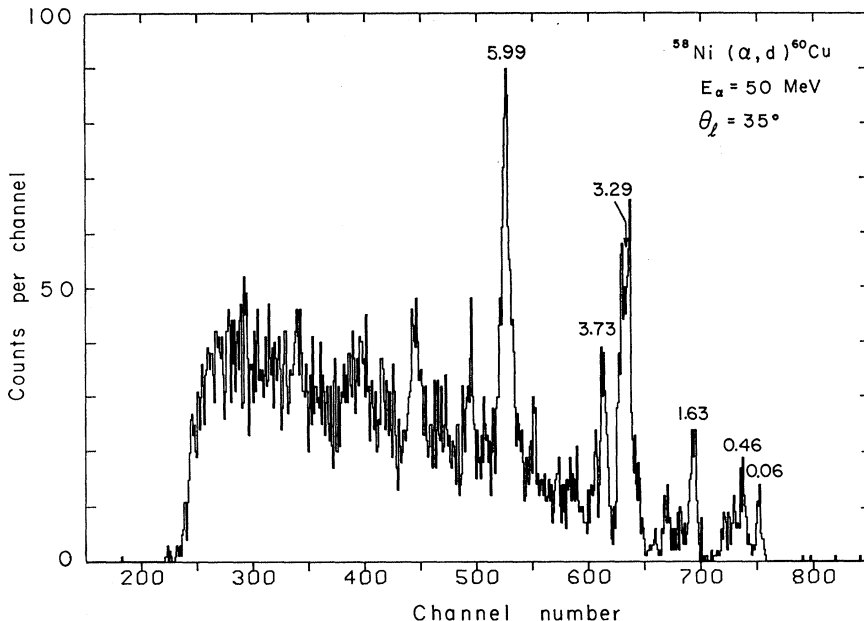


FIG. 12. Deuteron energy spectrum from the reaction $^{58}\text{Ni}(\alpha, d)^{60}\text{Cu}$ at a scattering angle of 35° (lab).

this mass region from $A=14$ to 26 with a value of about -3.9 MeV (i.e., attractive). Except for the nucleus ^{26}Al , the residual interaction decreases slightly with increasing A .

For $T_z \neq 0$ nuclei, the situation is more complicated. As an example, the $\frac{1}{2}^1_-, T=\frac{1}{2}$ state of ^{15}N , which is assumed to have the configuration

$$[(^{13}\text{C core})_{1/2^-, 1/2}(1d_{5/2})_{5+, 0^2}]_{11/2^-, 1/2},$$

will be discussed below.

The S_n value in Eq. (1) is equal to the neutron separation energy from the ^{13}C ground state in the ^{14}C state with configuration $(d_{5/2}, p_{1/2})_{3-, 1}$. The S_p value in Eq. (1) is equal to the mean value of the proton separation energy from the ^{13}C ground state

weighted by assuming that the probability in the $^{14}\text{N}(d_{5/2}, p_{1/2})_{3-, 0}$ state is a_J , and the probability in the $^{14}\text{N}(d_{5/2}, p_{1/2})_{3-, 1}$ is b_J . The probabilities a_J and b_J are obtained by requiring that the total interaction energy of the two $d_{5/2}$ nucleons in a configuration $(1d_{5/2})_{5+, 0^2}$ to the $p_{1/2}$ neutron of ^{13}C be equal to the sum of the interaction of the $d_{5/2}$ proton to the $p_{1/2}$ neutron and of the $d_{5/2}$ neutron to the $p_{1/2}$ neutron. That is,

$$\begin{aligned} \langle (1d_{5/2})_{5+, 0^2} p_{1/2} J = \frac{1}{2}^1_-, T = \frac{1}{2} \mid \sum_{i=1}^2 V_{i3} \mid \\ \times (1d_{5/2})_{5+, 0^2} p_{1/2} J = \frac{1}{2}^1_-, T = \frac{1}{2} \rangle \\ = [a_3 V_{3,0} + b_3 V_{3,1}] + V_{3,1}. \end{aligned}$$

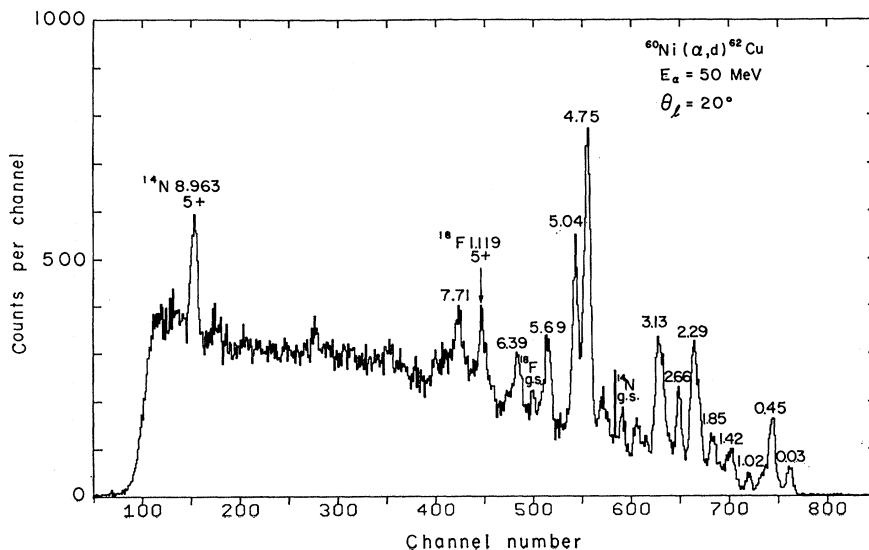


FIG. 13. Deuteron energy spectrum from the reaction $^{60}\text{Ni}(\alpha, d)^{62}\text{Cu}$ at a scattering angle of 20° (lab).

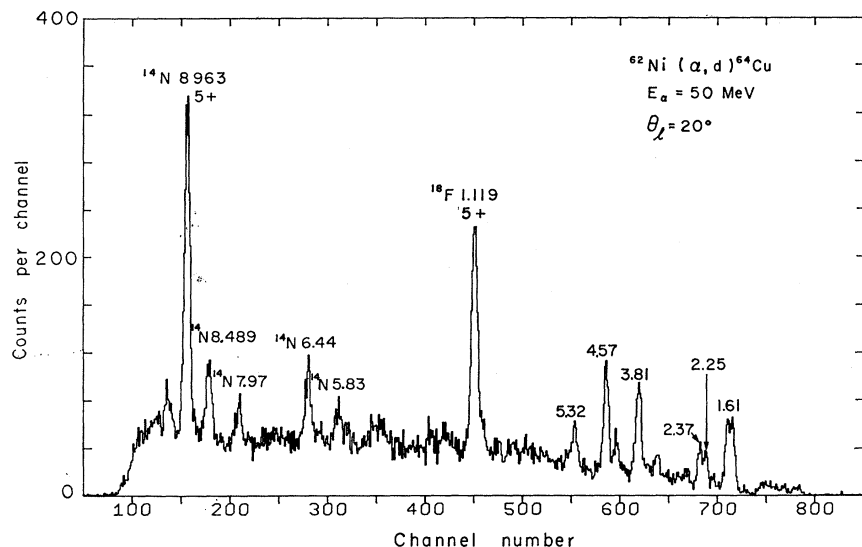


FIG. 14. Deuteron energy spectrum from the reaction $^{62}\text{Ni}(\alpha, d)^{64}\text{Cu}$ at a scattering angle of 20° (lab).

On the right-hand side of the above equation the notation $V_{J',T'}$ is used. The quantities in the brackets represent the neutron-proton interaction and the last term represents the neutron-neutron interaction. The quantity on the left-hand side of the above equation can be expressed in terms of two-body matrix elements $V_{J',T'}$ by applying Eq. (37.19) of Ref. 33. However, it must be noted that in the $(d_{5/2}, p_{1/2})_{3-0}$ or $(d_{5/2}, p_{1/2})_{3-1}$ state of ^{14}N , the proton is in the $d_{5/2}$ state half of the time while the proton in the $[(d_{5/2})_{5+,0^2}p_{1/2}]_{J,T}$ state of ^{15}N can only be in the $d_{5/2}$

state. Therefore, an additional Coulomb energy correction must be introduced. The Coulomb energy difference between a $d_{5/2}$ proton coupled to the ^{12}C core and a $p_{1/2}$ proton coupled to the ^{12}C core is just the difference of the excitation energy between the $d_{5/2}$ single-particle excited states of ^{13}C and ^{13}N , which are 3.85 and 3.56 MeV, respectively. This difference is equal to 0.29 MeV. The Coulomb energy correction is equal to half of this value, i.e., 0.15 MeV.

The above method was used to calculate the residual interaction for the ^{15}N (13.023-MeV), ^{17}O (7.743-MeV),

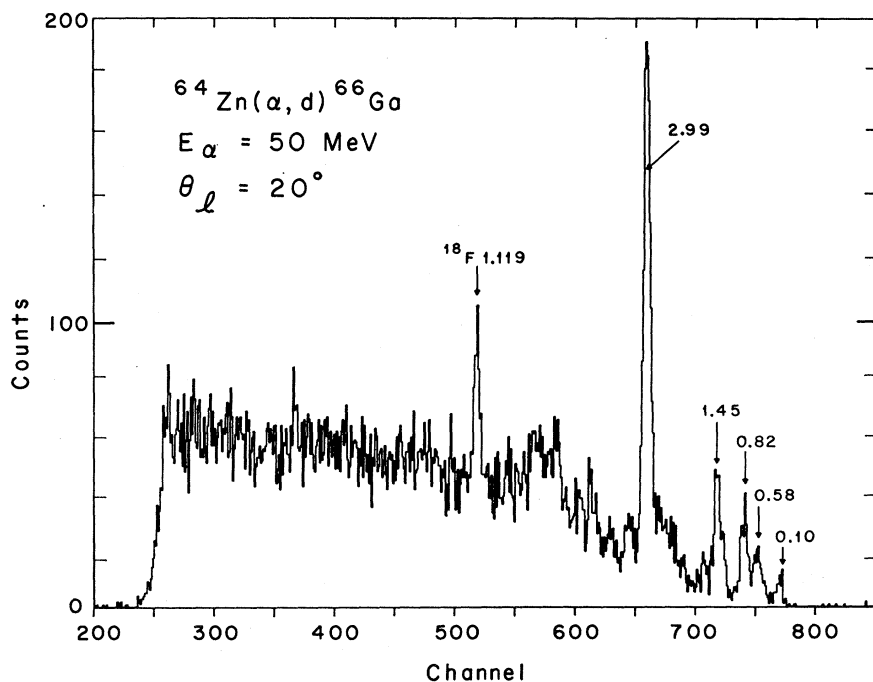


FIG. 15. Deuteron energy spectrum from the reaction $^{64}\text{Zn}(\alpha, d)^{66}\text{Ga}$ at a scattering angle of 20° (lab).

³³ A. de-Shalit and I. Talmi, *Nuclear Shell Theory* (Academic Press Inc., New York, 1963), p. 480.

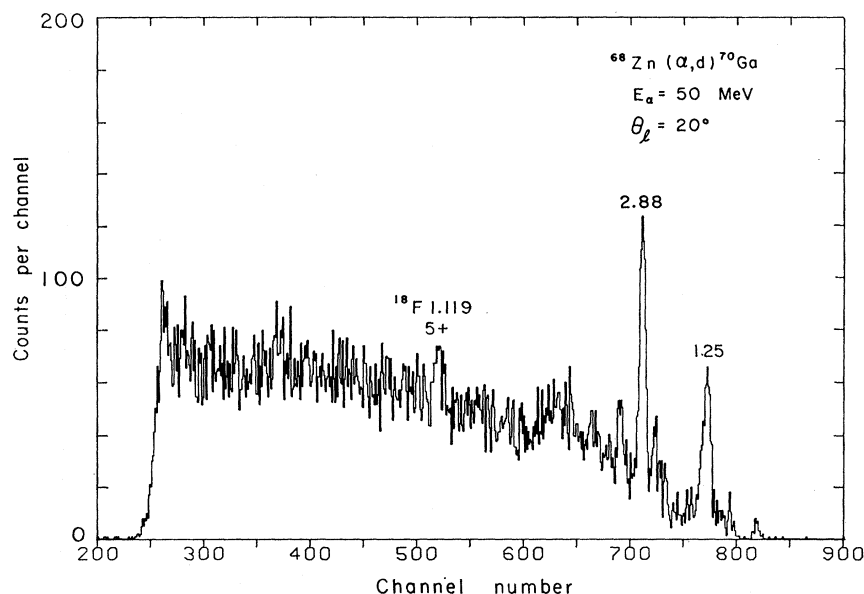


FIG. 16. Deuteron energy spectrum from the reaction $^{66}\text{Zn}(\alpha, d)^{70}\text{Ga}$ at a scattering angle of 20° (lab).

^{6}O (16.24-MeV), and ^{16}N (5.747-MeV) levels assuming that these states have spins $\frac{1}{2}^{\pm}$, $\frac{1}{2}^{\pm}$, 6, and 5, respectively. The Coulomb energy corrections are 0.15, 0.22, 0, and 0.13 MeV, respectively. The values obtained, as well as the level information of neighboring nuclides used, are listed in Table VII. The name "interaction model" is used to signify the present separation of interaction energy of $(1d_{5/2})_{5+,0^2}$ -to-core into proton-to-core and neutron-to-core interactions.

From (α, d) experiments, a level in each of the four

TABLE V. The $(1d_{5/2})_{5+,0^2}$ levels observed in the (α, d) reaction and their $-Q_f$ values.

Final nucleus	Energy of excitation (MeV)	$-Q_f$ (MeV)	$J\pi$	T
^{14}N	8.963 ± 0.002^a	22.54	$5+^a$	0
^{15}N	11.95 ± 0.02	19.64	$(9/2-)$	$\frac{1}{2}$
	13.03 ± 0.02	20.72	$(11/2-)$	$\frac{1}{2}$
^{16}N	5.75 ± 0.02	19.13	$(5+)$	1
^{16}O	14.39 ± 0.03^b	17.50	$(4, 5+)^c$	0
	14.81 ± 0.03^b	17.92	$(5, 4+)^c$	0
	16.24 ± 0.03^b	19.35	$(6+)^{c,d}$	0
^{17}O	7.74 ± 0.02	17.54	$(11/2-)$	$\frac{1}{2}$
	9.14 ± 0.03	18.94	$(9/2-)$	$\frac{1}{2}$
^{18}F	1.1310 ± 0.0015^e	17.45	$5+^f$	0
^{22}Na	1.5281 ± 0.0003^g	14.10	$5+^h$	0
^{26}Al	g.s.	12.43	$5+^i$	0

^a Reference 6.

^b Reference 4.

^c Assigned by this work.

^d This spin assignment, which is different from those in Ref. 3, will be discussed in Sec. IV C.

^e T. K. Alexander, K. W. Allen, and D. C. Hearly, Phys. Letters **20**, 402 (1966).

^f Reference 8.

^g E. K. Warburton, J. W. Olness, and A. R. Poletti, Phys. Rev. **160**, 938 (1967); A. R. Poletti, E. K. Warburton, J. W. Olness, and S. Hecht, *ibid.*, **162**, 1040 (1967).

^h Reference 9.

ⁱ P. M. Endt and C. van der Leun, Nucl. Phys. **A105**, 1 (1967).

$T_z=0$ nuclei ^{14}N , ^{18}F , ^{22}Na , and ^{26}Al was assigned spin-parity $5+$ and the configuration (core) $(1d_{5/2})_{5+,0^2}$. From independent work, each of these levels is known to have spin-parity $5+$. One may therefore safely assume that the main configuration is indeed (core) $(1d_{5/2})_{5+,0^2}$. Further, the experimental residual-interaction energies stay constant at about -3.9 MeV over the mass region $A=13$ to 26, as will be shown in Sec. IV D. This value of the $(1d_{5/2})_{5+,0^2}$ interaction energy is very reasonable, proving that the method used for the extraction of the interaction energies for the $T=0$ nuclei is correct. Since the calculation of the interaction energy for the $T_z \neq 0$ nuclei gives a result in excellent agreement with that obtained for the $T_z=0$ nuclei, one may have considerable confidence in the method of calculation as well as in the assignments of spins and parities for the levels of $T_z \neq 0$ nuclei shown in Table VII. Alternatively, an experimental verification of the spin of these states would prove the correctness of the above interaction-model approach used for the $T_z \neq 0$ nuclides.

One can expect that the above calculational method,

TABLE VI. High-spin [probably $(1g_{9/2})_{9+}^2$] levels observed in the (α, d) reaction.

Final nucleus	Energy level (MeV)	$-Q_f$ (MeV)
^{54}Mn	9.47 ± 0.05	20.04
^{56}Co	8.92 ± 0.03	19.85
^{58}Co	6.79 ± 0.03	18.27
^{60}Cu	5.99 ± 0.03	18.58
^{62}Cu	4.75 ± 0.03	17.12
^{64}Cu	4.57 ± 0.03	16.60
^{66}Ga	2.99 ± 0.03	16.00
^{68}Ga	2.88 ± 0.03	15.40
^{70}Ga	2.88 ± 0.03	14.69

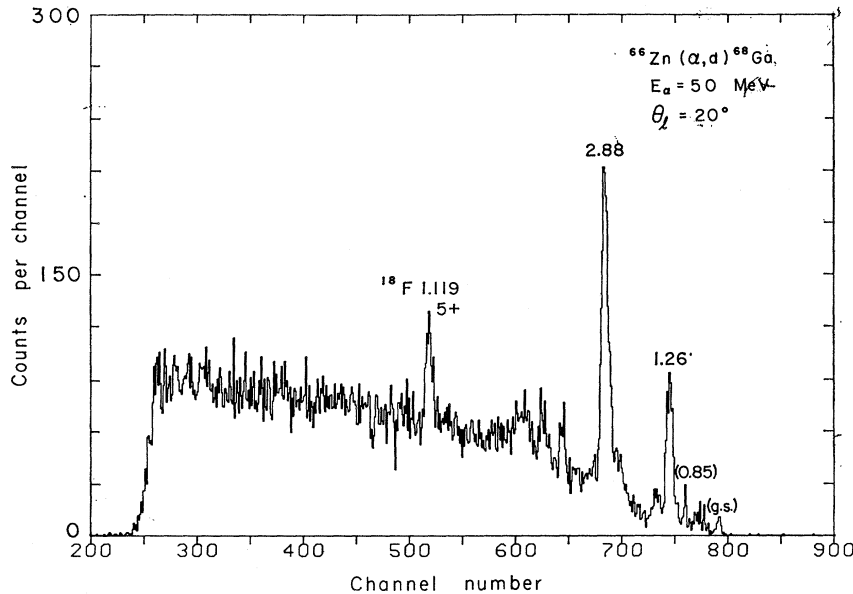


FIG. 17. Deuteron energy spectrum from the reaction $^{66}\text{Zn}(\alpha, d)^{68}\text{Ga}$ at a scattering angle of 20° (lab).

for both $T_z=0$ or $T_z \neq 0$ nuclides, is quite good on the following two accounts:

(a) Because of the high spin value of the state considered, configuration mixing is small.

(b) By using experimental energies of neighboring nuclei, some core excitation has already been taken into account. That is to say, the states of neighboring nuclei used in the calculation need not have a very pure configuration. As long as the presence of the additional $d_{5/2}$ nucleon of the two-particle state does not alter this configuration appreciably, the interaction energy thus calculated may still be accurate even though the true configuration of the target is not purely $[(^{12}\text{C core})(p_{1/2})^n]$.

Following the same method as discussed above, the residual-interaction energy between proton and neutron in the $(1f_{7/2})_{7+,0^2}$ configuration has been calculated. The results are listed in Table VIII. The excitation energies of the two-particle excited states used here are from Ref. 3. For ^{28}Al , the values of a_J and b_J are $\frac{2}{3}$ and $\frac{1}{3}$, respectively. The Coulomb energy correction is 0.11 MeV. The residual-interaction energy stays fairly constant but decreases slightly faster with increasing A as compared to the $(1d_{5/2})_{5+,0^2}$ residual-interaction energies.

Similarly, the interaction-model method can be applied to calculate the residual-interaction energies between proton and neutron in the $(1g_{9/2})_{9+,0^2}$ configuration. These calculations need the value of the excitation energies of the analog states. The single-particle $1g_{9/2}$ states in ^{59}Cu and ^{61}Cu analog to ^{59}Ni and ^{61}Ni are known.³⁴ The Coulomb displacement energies, E_C , of the ^{53}Mn , ^{55}Co , ^{63}Cu , and Ga (natural mixture of isotopes)

analog to the ground states of ^{53}Cr , ^{55}Fe , ^{63}Ni , and Zn are equal to 8.390, 8.660, 9.300, and 9.76 MeV, respectively.³⁵ The $1g_{9/2}$ analog states are assumed to have the same excitation energies above the analogs of the ground states of ^{53}Cr , ^{55}Fe , ^{63}Ni , ^{65}Zn , and ^{67}Zn as the excitation energies of the $1g_{9/2}$ single-particle states of the latter nuclei. Coulomb energy corrections are not included because there is not enough experimental information to calculate these values. This is justified from the previous calculations for $(1d_{5/2})_{5+,0^2}$ which have shown that these corrections are only about 150–220 keV.

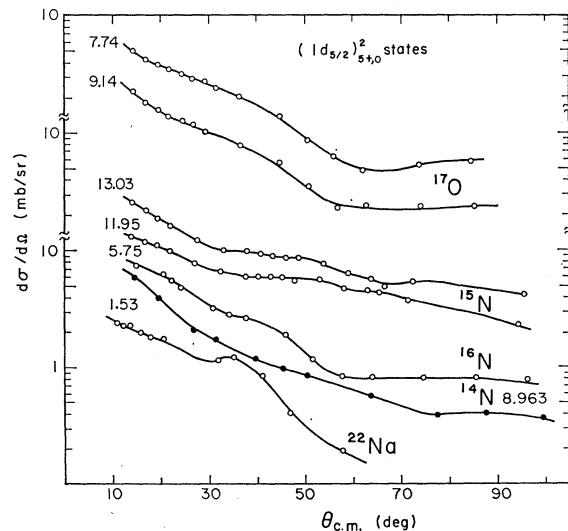


FIG. 18. Angular distributions of deuterons from (α, d) reactions to states of $(1d_{5/2})_{5+,0^2}$ configuration. The curves have no theoretical significance.

³⁴ A. G. Blair and D. D. Armstrong, Phys. Letters 16, 57 (1965); A. G. Blair, Los Alamos Scientific Laboratory Report No. LADC-6370, 1964 (unpublished).

³⁵ R. Sherr, Phys. Letters 24B, 321 (1967); J. D. Anderson, C. Wong, and J. W. McClure, Phys. Rev. 138, B615 (1965).

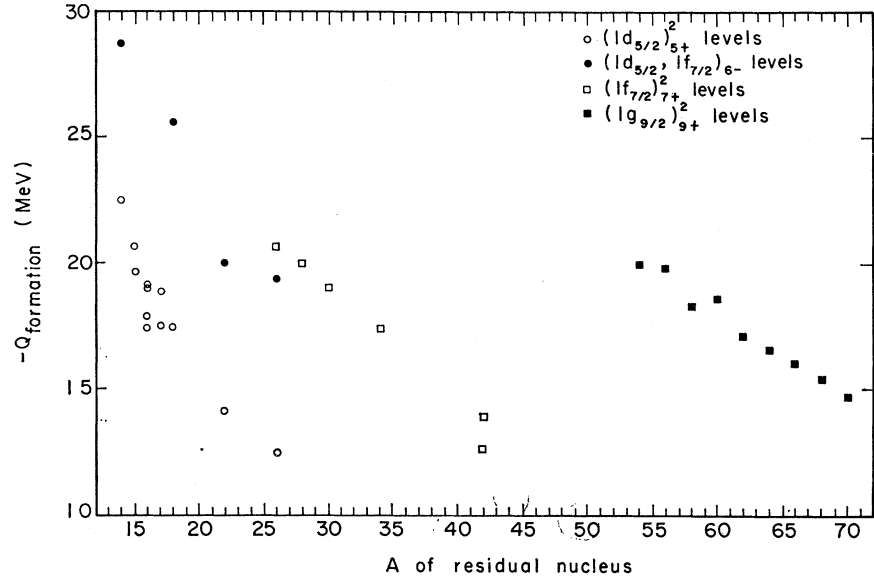


FIG. 19. Relationship between the mass number A of the product nucleus and the Q value of formation of levels with $(1d_{5/2})_{5+}^2$, $(1f_{7/2})_{7+}^2$, $(1d_{5/2}, 1f_{7/2})_{6-}$, and (probably) $(1g_{9/2})_{9+}^2$ configurations strongly populated by the (α, d) reaction.

The constants $a_{J'}$ and $b_{J'}$ for each nucleus are determined with the following assumption about the configuration of the ground state of the target core:

- ^{52}Cr : $(1f_{7/2})_{0+,2}^{12}$,
- ^{54}Fe : $(1f_{7/2})_{0+,1}^{14}$,
- ^{58}Ni : $(2p_{3/2})_{0+,1}^2$ or $(1f_{5/2})_{0+,1}^2$,
- ^{60}Ni : $(2p_{3/2})_{0+,2}^4$ or $(1f_{5/2})_{0+,2}^4$,
- ^{62}Ni : $(1f_{5/2})_{0+,3}^6$,
- ^{64}Zn : $(1f_{5/2})_{0+,2}^8$,
- ^{66}Zn : $(2p_{1/2})_{0+,0}^4(1f_{5/2})_{0+,3}^6$.

In all the cases thus calculated, the constants $a_{J'}$ and

$b_{J'}$ have the value

$$a_{J'} = 2T_i / (2T_i + 1), \quad b_{J'} = 1 / (2T_i + 1),$$

where T_i is the isobaric-spin quantum number of the target. The results of these calculations are listed in Table IX. For the nuclei ^{58}Co and ^{70}Ga , the target nuclei (^{56}Fe and ^{68}Zn) have to occupy two shell-model states [i.e., $(f_{7/2})^{-2}(p_{3/2})^{-2}$ or $(p_{3/2})^6(f_{5/2})^6$, respectively] beyond a closed $1f_{7/2}$ shell. Then, one needs to calculate the interaction energy between the $g_{9/2}$ nucleons and the j_1 and j_2 nucleons in the configuration

$$[(j_1)_{J_1 T_1}^{n_1} (j_2)_{J_2 T_2}^{n_2} (1g_{9/2})_{9+,0}^2]_{J, T}.$$

TABLE VII. Experimental residual-interaction energies for the $(1d_{5/2})_{5+,0}^2$ configuration.^a

	Two-particle excited states	Single-particle state		$E(1d_{5/2})_{5+,0}^2$ ^b		
		Assumed $1d_{5/2}$ neutron states	Assumed $1d_{5/2}$ proton states			
^{14}N :	8.963 5+ ^c	^{13}C :	3.85 5/2+ ^{d,e}	^{18}N :	3.56 5/2+ ^{d,e}	-4.05
^{18}F :	1.131 5+ ^f	^{17}O :	0.000 5/2+ ^{d,e}	^{17}F :	0.000 5/2+ ^{d,e}	-3.88
^{22}Na :	1.528 5+ ^g	^{21}Ne :	0.353 5/2+ ^h	^{21}Na :	0.338 5/2+ ⁱ	-3.47
^{26}Al :	0.000 5+ ⁱ	^{25}Mg :	0.000 5/2+ ⁱ	^{26}Al :	0.000 5/2+ ⁱ	-4.04
^{15}N :	13.03 (11/2-) ^j	^{14}C :	6.723 3-, $T=1^{e,k,l}$	^{14}N :	5.83 3-, $T=0^{d,e}$	-3.57 ^m
					8.90 3-, $T=1^{d,e}$	
					6.135 3-, $T=0^o$	-3.69 ^m
^{17}O :	7.74 (11/2-) ^j	^{16}N :	0.300 3-, $T=1^{e,n}$	^{16}O :	13.26 3-, $T=1^o$	
					7.28 (7/2+) ^p $l_n=2$	-3.44 ^m
^{18}O :	16.24 (6+) ^j	^{15}N :	7.57 7/2+ ^p	^{15}O :	5.276 5/2+, $T=1/2^p$	-3.82 ^m
^{16}N :	5.75 (5+) ^j	^{15}C :	0.75 5/2+, $T=3/2^{1,o}$	^{15}N :	12.502 5/2+, $T=3/2^q$	

^a All the energies are in units of MeV.
^b Experimental proton-neutron residual-interaction energy.
^c References 6, 7.
^d Reference 43.
^e Reference 36.
^f Reference 8.
^g Reference 9.
^h A. J. Howard, J. P. Allen, and D. A. Bromley, Phys. Rev. **139**, B1135 (1965).
ⁱ P. M. Endt and C. van der Leun, Nucl. Phys. **A105**, 1 (1967).

^j Assigned by this work.
^k R. K. Gupta and P. C. Sood, Phys. Rev. **152**, 917 (1966).
^l F. Ajzenberg-Selove and T. Lauritsen, Nucl. Phys. **11**, 1 (1959).
^m Calculated by using the interaction model discussed in the text.
ⁿ P. V. Hewka, C. H. Holbrow, and R. Middleton, Nucl. Phys. **88**, 561 (1966).
^o I. Kelson, Phys. Letters **16**, 143 (1965).
^p E. K. Warburton and J. W. Olness, Phys. Rev. **147**, 698 (1966); E. K. Warburton, J. W. Olness, and D. E. Alburger, *ibid.* **140**, B1202 (1965).
^q P. Loncke and J. Pradal, Nuovo Cimento **48B**, 457 (1967).

TABLE VIII. Experimental residual-interaction energies for the $(1f_{7/2})_{\tau+,0^2}$ configuration.^a

Two-particle excited states	Assumed $1f_{7/2}$ neutron states	Single-particle states ^b Assumed $1f_{7/2}$ proton states	$E(1f_{7/2})_{\tau+,0^2}$ ^c
²⁶ Al: 8.27	²⁵ Mg: 3.97 ($\frac{5}{2}, \frac{3}{2}$) ⁻ (<i>d, p</i>) $l_n=3$	²⁵ Al: 3.72 $\frac{7}{2}$ - b,d	-3.44
³⁰ P: 7.03	²⁹ Si: 3.623 $\frac{7}{2}$ - (<i>d, p</i>) $l_n=3$	²⁹ P: 3.44 $\frac{7}{2}$ - e,d (³ He, <i>d</i>), (<i>d, n</i>) $l_p=3$	-2.89
³⁴ Cl: 5.2	³³ S: 2.937 $\frac{7}{2}$ - (<i>d, p</i>) $l_n=3$	³³ Cl: (2.5) ^f	-(3.11)
⁴² Sc: 0.60	⁴¹ Ca: 0.000 $\frac{7}{2}$ - (<i>d, p</i>) $l_n=3$	⁴¹ Sc: 0.000 $\frac{7}{2}$ - (<i>t, d</i>), (<i>d, n</i>) $l_p=3$	-2.62
²⁸ Al: 9.80	²⁷ Mg: 3.575 ($\frac{3}{2}, \frac{5}{2}$) ⁻ $T=\frac{3}{2}$	²⁷ Al: 6.48 $\frac{7}{2}$ ($\frac{3}{2}$) ^{g,d} $T=\frac{3}{2}$ 10.50 $\frac{7}{2}$ - h $T=\frac{3}{2}$	-2.96

^a All the energies are in the units of MeV.

^b All the single-particle-state information is from P. M. Endt and C. van der Leun [Nucl. Phys. **A105**, 1 (1967)] if not otherwise indicated.

^c Experimental proton-neutron residual-interaction energy.

^d Our analysis of the (α, t) reaction data collected by R. Pehl, E. Rivet, J. Cerny, and B. G. Harvey showed that the g.s. $\frac{5}{2}+$ and 3.72-MeV $\frac{7}{2}-$ states of ²⁵Al, the 1.38-MeV $\frac{3}{2}+$ and 3.44-MeV $\frac{7}{2}-$ states of ²⁹P, and the g.s. $\frac{5}{2}+$, 2.98-MeV $\frac{3}{2}+$, and 6.48-MeV states of ²⁷Al were strongly populated.

^e H. Ejiri, T. Ishimatsu, K. Yagi, G. Breuer, Y. Nakajima, H. Ohmura,

T. Tohei, and T. Nakagawa, J. Phys. Soc. (Japan) **21**, 2110 (1966). The only known levels that could be the analog state of the ³³S 2.937-MeV $\frac{7}{2}$ state are the 2.5- and 2.979-MeV states. The former is more likely because systematic trends indicate that the odd-proton states usually have excitation energy less than the analog odd-neutron states.

^f C. van der Leun, D. M. Sheppard, and P. M. Endt, Nucl. Phys. **A100**, 316 (1967); D. M. Sheppard and C. van der Leun, *ibid.* **A100**, 333 (1967).

^g The average value of the two $\frac{7}{2}-$, $T=\frac{3}{2}$ states at 10.51 and 10.48 MeV in Ref. f was used.

Equation (37.19) of Ref. 33 is no longer adequate to treat this case. Hence, no calculation has been made for these two nuclides. Although configurations which may be different from the true ones are assumed for the g.s. of ⁶²Ni, ⁶⁴Zn, and ⁶⁶Zn, the calculated values may still be correct due to the second reason discussed above.

C. Calculation of Excitation Energies of States with the Configuration $(1d_{5/2})_{5+,0^2}$

One could use the following method to calculate the excitation energies of the $(1d_{5/2})_{5+,0^2}$ states for the nuclei ¹⁵N, ¹⁶N, ¹⁶O, and ¹⁷O. It is assumed that the residual-interaction energy of $(1d_{5/2})_{5+,0^2}$ stays constant

TABLE IX. Experimental residual-interaction energies for the $(1g_{9/2})_{9+,0^2}$ configuration (all energies in MeV).

Two-particle excited states	Assumed $1g_{9/2}$ neutron states	Single-particle states Assumed $1g_{9/2}$ proton states ^a	$E(1g_{9/2})_{9+,0^2}$ ^b
⁵³ Mn: 9.47	⁵³ Cr: 3.70 $\frac{9}{2}+$ ^c	⁵³ Mn: (6.4) ^d (10.72) ^e	-(2.49)
⁵⁶ Co: 8.92	⁵⁶ Fe: 3.80 $\frac{9}{2}+$ ^f	⁵⁶ Co: 6.01 $\frac{9}{2}+$ ^{d,g,h} (8.56) ^e	-(2.54)
⁶⁰ Cu: 5.99	⁵⁹ Ni: 3.07 $\frac{9}{2}+$ ⁱ	⁵⁹ Cu: 2.99 $\frac{9}{2}+$ ^{d,i} 6.86 ($\frac{9}{2}+$) ^o	-2.42
⁶² Cu: 4.75	⁶¹ Ni: 2.13 $\frac{9}{2}+$ ⁱ	⁶¹ Cu: 2.71 $\frac{9}{2}+$ ^{d,i} 8.56 ($\frac{9}{2}+$) ^e	-2.34
⁶⁴ Cu: 4.57	⁶³ Ni: 1.7 ^f (centroid)	⁶³ Cu: 2.51 $\frac{9}{2}+$ ^k (10.46) ^o	-(1.93)
⁶⁶ Ga: 2.99	⁶⁶ Zn: 1.04 $\frac{9}{2}+$ ^l	⁶⁶ Ga: 2.03 $\frac{9}{2}+$ ^{d,m} (7.10) ^o	-(2.22)
⁶⁸ Ga: 2.88	⁶⁷ Zn: 0.64 ^l	⁶⁷ Ga: 2.10 ^d (8.98) ^o	-(2.07)

^a Of the two excitation energies listed for each nucleus, the lower one is the analog $g_{9/2}$ state to the neutron $g_{9/2}$ state.

^b Experimental proton-neutron residual-interaction energy.

^c A. A. Rollefson, R. C. Barse, J. C. Legg, G. C. Phillips, and G. Roy, Nucl. Phys. **63**, 561 (1965).

^d (α, t) data in Ref. 31.

^e Analog states. See discussion in the text.

^f R. H. Fulmer and A. L. McCarthy, Phys. Rev. **131**, 2133 (1963).

^g B. J. O'Brien, W. E. Dorenbusch, T. A. Belote, and J. Rapaport, Nucl.

Phys. **A104**, 609 (1967); D. D. Armstrong and A. G. Blair, Phys. Rev. **140**, B1226 (1965); P. H. Vuister, Nucl. Phys. **A91**, 521 (1967).

^h B. Rosner and C. H. Holbrow, Phys. Rev. **154**, 1080 (1967).

ⁱ Reference 21.

^j Reference 34.

^k A. G. Blair, Phys. Rev. **140**, B648 (1965).

^l References 25 and 26.

^m M. G. Betigeri, H. H. Duhm, R. Santo, R. Stock, and R. Bock, Nucl. Phys. **A100**, 416 (1967).

over this mass region and has a value of -3.90 MeV. Then one uses Talmi's method with the change that the $(d_{5/2}p_{1/2})$ interaction energies (i.e., $V_{3,0}$, $V_{2,0}$, $V_{3,1}$, and $V_{2,1}$) are expressed in terms of excitation energies of certain states of neighboring nuclei that can also be expressed in terms of $(d_{5/2}p_{1/2})$ interaction energies.

In the calculations for ^{16}N , the 0.75 -MeV $\frac{5}{2}^+$, $\frac{3}{2}^+$ level of ^{15}C and the 5.276 -MeV $\frac{5}{2}^+$, $\frac{1}{2}^+$ and 12.502 -MeV $\frac{5}{2}^+$, $\frac{3}{2}^+$ levels of ^{15}N are assumed to be the J, T states of the configuration $[(p_{1/2})_{0,1}^2 d_{5/2}]_{J,T}$, where $J = \frac{5}{2}$ and $T = \frac{1}{2}$ or $\frac{3}{2}$. For ^{16}O , the 7.563 -MeV $\frac{7}{2}^+$, $\frac{1}{2}^+$ and 7.154 -MeV $\frac{5}{2}^+$, $\frac{1}{2}^+$ levels of ^{15}N and the 7.28 -MeV $\frac{7}{2}^+$, $\frac{1}{2}^+$ and 6.86 -MeV $\frac{5}{2}^+$, $\frac{1}{2}^+$ levels of ^{15}O are assumed to be the J, T states of the configuration $[(p_{1/2})_{1,0}^2 d_{5/2}]_{J,T}$ with $J = \frac{7}{2}$ or $\frac{5}{2}$ and $T = \frac{1}{2}$. For ^{17}O , the 6.13 -MeV $3^-, 0$, 8.88 -MeV $2^-, 0$, 13.26 -MeV $3^-, 1$, and 12.97 -MeV $2^-, 1$ levels of ^{16}O and the ground-state $2^-, 1$ and 0.300 -MeV $3^-, 1$ levels of ^{16}N are assumed to be the J, T states of the configuration $(p_{1/2}^{-1} d_{5/2})_{J,T}$, with $J = 3$ or 2 and $T = 0$ or 1 . The results are presented in Fig. 20.

Comparable but less accurate results are obtained for the levels using Talmi and Unna's empirical matrix elements.³⁶ The results are shown in Fig. 21.

Because the first method uses the excitation energies of neighboring nuclides which may contain some core excitation, this method will give better agreement to the experimental value if the target has a core-excitation component [i.e., cannot be represented as a simple $(p_{1/2})^n$ configuration]. For example, recent analysis of core-polarization effects in ^{15}N - ^{15}O by Brown and Shukla suggest that there may be 10% of 2p-3h components in the ground-state wave function of ^{15}N or ^{15}O .³⁷ If, on the other hand, there is a considerable fragmentation of single-particle strength in the $A+1$ nuclei, then associating the configuration with only one state may also be inappropriate.

The ordering of the triplet in ^{16}O is interesting. Previous experimental work³ suggested that the ordering of the states might be 4^+ , 6^+ , and 5^+ based

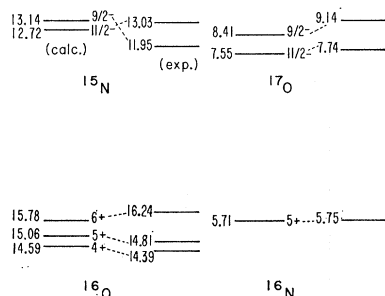


Fig. 20. Comparison between the experimental excitation energies of the $(1d_{5/2})_{5+,0^2}$ levels and the theoretical values using the level information from neighboring nuclides.

³⁶ I. Talmi and I. Unna, *Ann. Rev. Nucl. Sci.* **10**, 353 (1960).
³⁷ G. E. Brown and A. P. Shukla, Princeton University Report No. PUC-937-268, 1967 (unpublished).

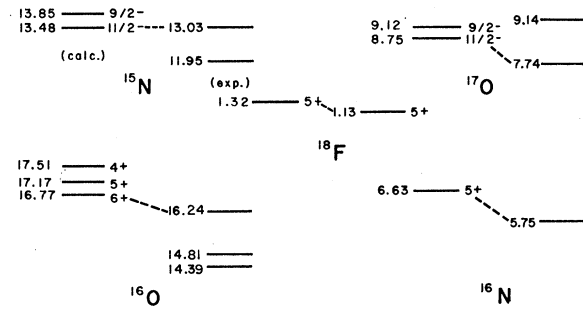


Fig. 21. Comparison between the experimental excitation energies of the $(1d_{5/2})_{5+,0^2}$ levels and the theoretical values using Talmi's method for the shell-model calculation.

on the $2J+1$ rule. However, the $2J+1$ rule is not followed for the doublet levels of both ^{15}N and ^{17}O strongly populated with the (α, d) reaction. This is perhaps not unexpected since, particularly for the lowest-spin member of a multiplet, configuration mixing is generally possible. In ^{16}O there are quite a few known 4^+ states and at least one 6^+ state³⁸ (at 16.2 MeV) which could possibly mix with the 2p-2h states observed in the (α, d) reaction. Recently the $^{14}\text{N}(\alpha, d)^{16}\text{O}$ experiment was repeated⁴ at $E_\alpha = 40$ MeV. With much better resolution than the previous experiment,³ a state at 15.8 MeV, unobserved in the earlier work, was found to be contributing to the cross section of the 16.24-MeV state. Thus, the agreement with the $2J+1$ rule was only apparent. The excitation energies used here are those from Ref. 4.

The known 6^+ in this region was identified by Carter *et al.*³⁸ as a member of a 4p-4h rotational band built on the 6-MeV 0^+ state. It has also been observed in the four-particle transfer $^{12}\text{C}(^6\text{Li}, d)^{16}\text{O}$ reaction.³⁹ However, Carter *et al.*³⁸ quote a width of 380 keV for the 4p-4h 6^+ state at 16.2 MeV, with a lower limit of 200 keV.⁴⁰ Our data⁴ indicate that the strong state observed in the (α, d) reaction at 16.24 MeV has a width almost surely less than 200 keV, which seems inconsistent with associating it with the 16.2-MeV 4p-4h 6^+ state.

Zuker *et al.*⁴¹ have done a shell-model calculation of the levels of ^{16}O using a closed ^{12}C core and considering particles in the $1p_{1/2}$, $1d_{5/2}$, and $2s_{1/2}$ shells. They found a 4p-4h 6^+ state (presumably that of Carter *et al.*³⁸) at 17.4 MeV and a triplet of levels of configuration

$$[(^{12}\text{C})_{0+,0}(p_{1/2})_{1+,0^2}(d_{5/2})_{5+,0^2}]_{4,5,6+,0},$$

³⁸ E. B. Carter, G. E. Mitchell, and R. H. Davis, *Phys. Rev.* **133**, B1421 (1964); E. B. Carter, *Phys. Letters* **27B**, 202 (1968).

³⁹ K. Meier-Ewert, K. Bethge, and K.-O. Pfeiffer, *Nucl. Phys.* **A110**, 142 (1968).

⁴⁰ E. B. Carter, Trinity University (private communication).

⁴¹ A. P. Zuker, B. Buck, and J. B. McGrory, *Phys. Rev. Letters* **21**, 39 (1968).

TABLE X. Comparison between theoretical and experimental proton-neutron residual-interaction energies of $(1d_{5/2})_{5+}^2$ configuration.

Nucleus	ν_1 (F ⁻²)	Shell-model calculation ^a		E_2	Experimental ^b $E(1d_{5/2})_{5+}^2$
		E_1	ν_2 (F ⁻²)		
¹⁴ N	0.326	-4.601	0.306	-4.291	-4.05
¹⁵ N	0.318	-4.481	0.299	-4.177	-3.57
¹⁶ N	0.311	-4.365	0.292	-4.068	-3.82
¹⁶ O	0.311	-4.365	0.292	-4.068	-3.44
¹⁷ O	0.304	-4.258	0.285	-3.968	-3.69
¹⁸ F	0.298	-4.165	0.280	-3.880	-3.88
²² Na	0.278	-3.847	0.261	-3.582	-3.47
²⁶ Al	0.262	-3.601	0.246	-3.349	-4.04

^a The choice of ν 's is discussed in the text. All the energies are in units of MeV.

^b From Table VII.

which were relatively pure. Their wave functions⁴² indicate that the states are 6+ (14.9 MeV), 5+ (15.5 MeV), and 4+ (16.19 MeV). The 7+ wave function has about 20% 4p-4h mixed with the dominant 2p-2h configuration, while the 5+ and 6+ states are more pure, having only about 5% 4p-4h admixture.⁴²

Our own calculations suggest that the state observed experimentally at 16.24 MeV is the 6+ member of the 2p-2h triplet. Unless the lower limit quoted by Carter⁴⁰ for the width of the 4p-4h 6+ state is wrong, there would therefore be two 6+ states very close in energy and relatively unmixed. This seems unlikely, so perhaps our assignment of spin 6+ to the 16.24-MeV state is incorrect.

D. Shell-Model Calculations

Conventional shell-model calculations were also used to calculate the residual-interaction energies between proton and neutron in the configurations $(1d_{5/2})_{5+}^2$, $(1f_{7/2})_{7+}^2$, and $(1g_{9/2})_{9+}^2$. In these calculations only a triplet-even potential is needed. This was taken from Ref. 43 and is equal to

$$V_{TE} = -52 \exp(-0.2922r^2) \text{ MeV.}$$

Tables X–XII list the results of these calculations for the above-mentioned three configurations, respectively. Two sets of harmonic-oscillator parameters ν (i.e., ν_1 and ν_2) are used. Within each set, the ν values for the nuclei ¹⁸F, ⁴²Sc, and ⁶⁶Ga were fixed first. The other ν 's for states with the same configuration were obtained by assuming an inverse dependence on $A^{1/3}$. The ν_1 values for the nuclei ¹⁸F, ⁴²Sc, and ⁶⁶Ga were calculated according to the equation⁴⁴

$$\nu_1 = (2n + l - \frac{1}{2}) / R^2,$$

where n, l are the principal quantum number and orbital angular momentum of the shell-model state concerned, respectively, and R is its rms radius. For

¹⁸F and ⁴²Sc, R was assumed to be the same as the equivalent uniform radius of $A=17$ and $A=41$ nuclei obtained from the Coulomb energy difference of mirror nuclei.⁴⁵ The ν_1 value of ⁶⁶Ga was fixed by first calculating a ν_1 value for ⁷³Ge (the first $1g_{9/2}$ neutron) using the above equation with R calculated from Eq. (1) of Ref. 35 and then taking an inverse proportionality to $A^{1/3}$. The ν_2 values of ¹⁸F and ⁶⁶Ga were obtained by adjusting their values such that they gave the same residual-integration energies as the experimentally calculated values. The ν values which are calculated from the often-used formula $\hbar\omega = 41A^{-1/3}$ give too-strong interaction energies and were not used here.

Comparison of the theoretical results thus obtained for the residual-interaction energy with the experimentally extracted values allows the conclusion that the agreement is, in general, satisfactory. A reasonably slight adjustment of ν 's (the second set) for $(1d_{5/2})_{5+}^2$ and $(1g_{9/2})_{9+}^2$ configuration gives excellent agreement, while no adjustment is needed for the ν 's of the $(1f_{7/2})_{7+}^2$ configuration. Kuo and Brown have calculated the residual-interaction energy between proton and neutron in the configuration $(1d_{5/2})_{5+}^2$ for the nucleus ¹⁸F (Ref. 46) and both $(1f_{7/2})_{7+}^2$ and $(1g_{9/2})_{9+}^2$ for ⁴²Sc (Ref. 47) from a free nucleon-

TABLE XI. Comparison between theoretical and experimental proton-neutron residual-interaction energies of the $(1f_{7/2})_{7+}^2$ configuration.

Nucleus	Shell-model calculation ^a		Experimental ^b $E(1f_{7/2})_{7+}^2$
	ν_1 (F ⁻²)	E	
²⁶ Al	0.276	-3.150	-3.44
²⁸ Al	0.269	-3.064	-(2.96)
³⁰ P	0.262	-2.980	-2.89
³⁴ Cl	0.251	-2.836	-(3.11)
⁴² Sc	0.234	-2.614	-2.62

^a The choice of ν 's is discussed in the text. All the energies are in units of MeV.

^b From Table VIII.

⁴² A. P. Zuker, Brookhaven National Laboratory (private communication).

⁴³ W. W. True, Phys. Rev. **130**, 1530 (1963).

⁴⁴ M. G. Redlich, Phys. Rev. **99**, 1427 (1955).

⁴⁵ L. R. B. Elton, *Nuclear Sizes* (Oxford University Press, Oxford, England, 1961), p. 56.

⁴⁶ T. T. S. Kuo and G. E. Brown, Nucl. Phys. **85**, 40 (1966).

⁴⁷ T. T. S. Kuo and G. E. Brown, Nucl. Phys. **A114**, 241 (1968).

TABLE XII. Comparison between theoretical and experimental proton-neutron residual-interaction energies of the $(1g_{9/2})_{9+,0^2}$ configuration.

Nucleus	ν_1 (F^{-2})	Shell-model calculation ^a		E_2	Experimental ^b $E(1g_{9/2})_{9+,0^2}$
		E_1	ν_2 (F^{-2})		
⁵⁴ Mn	0.226	-2.198	0.244	-2.400	-(2.49)
⁵⁶ Co	0.224	-2.167	0.241	-2.366	-(2.54)
⁶⁰ Cu	0.219	-2.111	0.236	-2.303	-2.42
⁶² Cu	0.216	-2.083	0.233	-2.275	-2.34
⁶⁴ Cu	0.214	-2.059	0.231	-2.247	-(1.93)
⁶⁶ Ga	0.212	-2.033	0.228	-2.221	-(2.22)
⁶⁸ Ga	0.209	-2.008	0.226	-2.195	-(2.07)

^a The choice of two sets of ν 's is discussed in the text. All the energies are in units of MeV.

^b From Table IX.

nucleon scattering potential (i.e., the Hamada-Johnston potential). The results, -3.69 , -2.199 , and -1.840 MeV for the three configurations, are in agreement with the experimentally calculated values as well as with the values obtained from conventional shell-model calculations. Their wave function for the $7+$, $T=0$ state of ⁴²Sc is⁴⁷

$$1.0(1f_{7/2})_{7+,0^2} - 0.07(1g_{9/2})_{7+,0^2},$$

which supports the postulate³ that this $7+$ state has dominant configuration

$$[(^{40}\text{Ca core})(1f_{7/2})_{7+,0^2}]_{7+,0}.$$

These results indicate that the assignments of states with pure configuration $(1d_{5/2})_{5+,0^2}$, $(1f_{7/2})_{7+,0^2}$, and $(1g_{9/2})_{9+,0^2}$ made in the last section and previous work³ are reasonable.

V. CONCLUSIONS

From the evidence presented in the previous section the following can be concluded:

(a) The systematic trend of (α, d) reactions at α -particle energy 40–50 MeV to populate strongly the states with a $(j)_{2j+,0^2}$ configuration still persists in the medium-region nuclides studied.

(b) States with configuration $[(\text{target core})(1g_{9/2})_{9+,0^2}]$ are located.

(c) States with configuration $[(\text{target core})(1d_{5/2})_{5+,0^2}]$ of ¹⁵N, ¹⁶N, ¹⁷O, and ²²Na are located.

(d) The residual-interaction energies between proton and neutron in the configurations $(1d_{5/2})_{5+,0^2}$, $(1f_{7/2})_{7+,0^2}$, and $(1g_{9/2})_{9+,0^2}$ are about -3.9 , -3.0 , and -2.2 MeV, respectively. There is a slight decrease of these residual-interaction energies with increasing A for all three configurations. The magnitudes of these residual-

interaction energies and their variation with A are reproduced satisfactorily by conventional shell-model calculations.

(e) The “interaction-model” method used to extract from the experimental results the residual-interaction energies for $T_z \neq 0$ nuclides is believed to be good, because it generates residual-interaction energies which are in agreement both with those obtained for $T_z = 0$ nuclides, and with the results obtained by the shell-model calculations. This method, which uses the excitation-energy information of nuclei with mass number A to calculate the residual-interaction energies or excitation energies of levels in the nucleus with mass number $A+1$, is believed to be more accurate than the method which tries to get a set of matrix elements from fitting the excitation energies of nuclides with a wider range of A .

(f) The 16.24-MeV level of ¹⁶O has a dominant 2p-2h configuration $[(^{14}\text{N g.s.})_{1+,0}(1d_{5/2})_{5+,0^2}]_{4,5,6+,0}$ and may have a spin-parity $6+$. Experimental determination of the spin of this state is needed in order to confirm this assignment.

The identification of the configuration of those states which are populated with medium cross sections in the (α, d) reaction by establishing systematic trends, spin and parity determination, and shell-model calculation will be very interesting.

ACKNOWLEDGMENTS

We are deeply indebted to Dr. Martin G. Redlich for many fruitful discussions. We would like to thank Dr. Nolan F. Mangelson for his invaluable help in the experimental work and Dr. W. W. True for allowing us to use his computer code for the matrix-element calculations.